END
DATE
FILMED
4-79

DDC

MICROCOPY RESOLUTION TEST CHART

NATIONAL BUREAU OF

LEVEL II

ⓘ

ADA064419

GLOW DISCHARGE OPTICAL SPECTROSCOPY

OF ION IMPLANTED GALLIUM ARSENIDE

THESIS

AFIT/GE/EE/78-D   Kenneth R. Williamson
                   Capt   USAF

D D C

A

79 01 30 145

⑥ GLOW DISCHARGE OPTICAL SPECTROSCOPY

OF ION IMPLANTED GALLIUM ARSENIDE.

THESIS ⑨ Master's thesis

Presented to the Faculty of the School of Engineering

of the Air Force Institute of Technology

Air Training Command

in Partial Fulfillment of the

Requirements for the Degree of

Master of Science ⑫ 74 p'

by

⑩ Kenneth R. Williamson, B.S.

Capt   USAF

Graduate Electrical Engineering

⑪ December 1978

Preface

In this report I have presented the results of an
experimental study of measuring impurity concentration
profiles of annealed and unannealed ion implanted gallium
arsenide (GaAs) by the glow discharge optical spectroscopy
(GDOS) technique. I hope that my efforts in calibration
of the GDOS system by use of pure elements will lead to
continued investigation and development of the system as
a useful total impurity concentration profiling technique.

I would like to thank the Avionics Laboratory personnel
for their assistance and guidance, including Dr. Y.S. Park
and 1Lt Bill Theis, my laboratory research advisor. Other
laboratory personnel who were extremely helpful were Jim
Ehret, Charlie Geesner, and Rick Patton. Thanks also to
Professor Seung Yun of Ohio State University for his help
in teaching me to operate the GDOS apparatus.

I would also like to thank Capt M. Borky, my thesis
advisor, for his assistance and for allowing me to "choose
my own path" in this experimental study. Special thanks
also to my wife for patience and help in preparing this
manuscript.

Contents

Contents

List of Figures

List of Figures

Abstract

Glow Discharge Optical Spectroscopy (GDOS) was used as a technique for obtaining impurity concentration profiles of annealed and unannealed ion implanted GaAs samples. Germanium, magnesium, and boron ions were implanted at energies of 60keV or 120keV and fluences of $1 \times 10^{15}/cm^2$ or $5 \times 10^{15}/cm^2$. One boron sample was implanted at energies of 60keV and 120keV. The samples were slowly eroded by cathode sputtering in a low-pressure dc glow discharge in an argon gas atmosphere. Strong emission lines were monitored as a function of time. The intensities of the emission lines (proportional to concentration) were calibrated using pure elements as standards, providing impurity concentration profiles.

GLOW DISCHARGE OPTICAL SPECTROSCOPY
OF ION IMPLANTED GALLIUM ARSENIDE

I Introduction

Background

Ion Implantation is becoming increasingly important
in fabricating semiconductor devices with higher electron
mobilities and band gaps than devices currently being
made from silicon or germanium. One semiconducting com-
pound, gallium arsenide, is being investigated extensively
by the Air Force Avionics Laboratory because it displays
these desired properties. Conventional diffusion doping
is extremely limited when using GaAs, whereas tailored
impurity profiles can be obtained using ion implantation.

The impurity profile must be accurately determined in
order to effectively use ion implantation in device fabri-
cation. Because the energy and amount of impurity can be
precisely measured during implantation, impurity profiles
can be repeatedly duplicated. The profile is a compli-
cated function of impurity energy and mass, substrate, and
crystal orientation, but can be accurately predicted for
most elements (Ref 2:1-39).

Ion implantation produces a substantial amount of
crystal lattice disorder, or damage. A crystal surface
may become amorphous during a high dose implant. The

crystal damage may be repaired by annealing the crystal at high temperatures. Implanted impurities can diffuse during annealing, thus altering the impurity profile.

Several methods of measuring impurity profiles are currently being used. Secondary Ion Mass Spectroscopy (SIMS) and Auger Spectroscopy both provide excellent depth resolution but both require expensive and elaborate equipment. Another method is to etch successive thin layers of substrate and then measure Hall coefficient or resistivity after each etch. The profile obtained yields an average over the total substrate etched and is not a direct measurement of the impurity distribution. Differential capacitance voltage (C-V) measurements, when properly analyzed, can yield profiles of implanted impurities. However this method is extremely limited for rapidly changing profiles such as are characteristic of implanted impurities.

Objectives

The purpose of this thesis was to evaluate Glow Discharge Optical Spectroscopy (GDOS) as a technique for measuring Magnesium implanted GaAs and to study the effects of annealing on the impurity profiles. The thesis was further expanded to include Germanium and Boron implanted GaAs.

The implanted substrate of interest is slowly dc sputtered in argon. During the sputtering excited atoms

are emitted and then spontaneously decay, emitting light
of characteristic wavelength. By accurately determining
the sputtering rate and by monitoring the discharge as
a function of time, an impurity profile can be obtained.

Results

Impurity concentration profiles were obtained for
germanium, magnesium, and boron implanted samples.
Profiles for Ge and B implants agreed favorably with the
theoretical LSS profiles. Flattening and spreading of the
measured curves were observed for annealed samples as
expected.

Magnesium implanted sample profiles basically followed
the LSS curves but were one and a half orders of magnitude
lower than the predicted values. Very high surface concen-
trations were observed for all samples capped with pyro-
lytic Si_3N_4 caps. Possible explanations for these devia-
tions from theory are discussed in Chapter VI.

Organization of Report

The second section of this report discusses the theory
of ion implantation and its advantages. Section III de-
scribes GDOS and its applications. The fourth section
gives a detailed description of the apparatus used in the
experiments, since the equipment is somewhat unique and by
no means standard. Section V discusses the procedure used
in performing the experiments along with the calibration
procedure used. Section VI is a summary of the results

3

obtained for each of the three implants. Included in this
section are graphic results obtained showing a comparison
to applicable theory. The last section gives the conclu-
sions drawn from the experiments as well as recommendations
for improvements to the GDOS system.

II Ion Implantation

History

Ion implantation is the process of bombarding a substrate with high energy ions. This bombardment or doping produces a spatial distribution or doping profile characteristic of the incident ion.

The first attempt to implant conventional dopants into semiconductors was done by Cussins in 1955 (Ref 1:296). He implanted a wide variety of ions into both single-crystal and amorphous germanium targets, and was able to obtain a p-type conductivity which apparently disappeared after a $500^{\circ}C$ anneal. Cussins concluded that the principal effect of the bombardment was the disruption of surface layers of the germanium lattice. Since this time several theories have been developed to predict implanted ion distribution in amorphous targets.

The theory that best predicts this distribution is the Lindhard, Scharff, and Schiott (LSS) range distribution theory (Ref 2:1-39). The LSS theory neglects sputtered surface atoms and assumes that the target is amorphous or is a crystalline target misaligned with respect to any high symmetry directions.

At present, a widely accepted method of implanting semiconductor crystals such as gallium arsenide is to purposely misalign the target 7° from the normal. The desired dopant species is first ionized in a beam-forming

electrode system. The extracted beam is then passed through a mass spectrometer magnet tuned to the mass of the desired ion species. The beam is then electrostatically accelerated into the target chamber where it is again accelerated to the final energy required. This entire system is kept under a very high vacuum to prevent the deflection of the desired ion beam by stray molecules. Provisions are also made to heat the target substrate since it has been found that higher doping efficiency (fraction of implanted ions which become electrically active) can be realized by hot implantations.

Energy Loss Equation

Energetic ions entering a target will, through collisions with the target nuclei and electrons, lose their energy and finally come to rest. These two forms of energy loss are usually assumed to be independent of each other. The result of this assumption is that for a single incident projectile the average rate of energy loss per path length is given by

$$-dE/dx = N\left[S_n(E) + S_e(E)\right] \tag{1}$$

where E is the energy of the particle at a point x along its path, $S_n(E)$ is the nuclear stopping power, $S_e(E)$ is the electronic stopping power, and N is the average number of target atoms per unit volume (Ref 1:298).

Nuclear stopping is assumed to be a two body elastic

6

scattering process and can be treated with classical
mechanics (Ref 3:11). In a crude first approximation, the
nuclear stopping power is independent of the projectile
energy and is only a function of the atomic number and
masses of the interacting particles. This approximation
can be written is the form

$$S_n(E) = 2.8 \times 10^{-15} \frac{Z_1 Z_2}{(Z)^{1/3}} \frac{M_1}{M_1 + M_2} \text{ eV cm}^2 \qquad (2)$$

where $\qquad Z^{1/3} = \left[Z_1^{2/3} + Z_2^{2/3} \right]^{1/2} \qquad (3)$

and where Z_1 and M_1 are the atomic number and mass of the
projectile, and Z_2 and M_2 are those of a target atom
(Ref 1:299). Nuclear stopping predominates for heavy ion,
low energy implants such as boron.

To obtain an approximation for the electronic stopping
power, the electrons in the target are considered as forming
a free electron gas. Lindhard and Wither (Ref 1:299)
have shown that the stopping power of a free electron gas
is proportional to the velocity of the projectile under
certain conditions. This approximation can be written as

$$S_e(E) = cv = kE^{1/2} \qquad (4)$$

where v and E are the velocity and energy of the projectile,
and k is a constant which depends on both the projectile
and the target material. This approximation of electronic
stopping power is used in the LSS calculations.

7

A somewhat different approximation of $S_e(E)$ has been proposed by Firsov (Ref 1:303). Similar to the nuclear stopping calculation, this approximation assumes a two-body collision between particles of charge z_1 and z_2. The computation of $S_e(E)$ is thus reduced to the computation of the energy transferred due to electronic interactions as the two particles approach each other and then separate. However, this approximation does not account for screening effects of tightly bound electrons, and in practice, $S_e(E)$ is usually found experimentally since neither of the above approximations completely describes the interaction.

Electronic stopping predominates for light ion, high energy implants such as magnesium. Nuclear and electronic stopping powers are considered by the LSS theory for an amorphous target only. The crystalline structure of a semiconcudtor material such as gallium arsenide thus complicates the theory for implantation along crystallographic planes.

Range Estimates

When the nuclear and electronic stopping powers are known, the average total range R that a projectile of initial energy E_0 will travel before coming to rest is given by

$$R = \int_0^R dx = \frac{1}{N} \int_0^{E_0} dE \Big/ \Big[S_n(E) + S_e(E) \Big] \qquad (5)$$

The projection of this distance R onto the direction of

8

incidence is called the projected range R_p and can be determined experimentally (Ref 1:299). The relationship between R and R_p is shown in Figure 1.

Because both the number of collisions and the energy transferred per collision are random, all ions of a given type and energy do not have the same range and instead exhibit a range distribution. A useful description of this distribution is the standard deviation of the projected range, R_p. Projected ranges and their standard deviations are tabulated for the ions and substrate used in this thesis research (Ref 9).

The impurity distribution of implanted ions, according to the LSS theory, is described by a gaussian function (Ref 4:87-126). For a given implant and substrate the peak concentration is given by

$$N_p = \frac{\emptyset}{\sqrt{2\pi}\Delta R_p} \qquad (6)$$

where $\emptyset$ is the fluence or dose (cm^{-2}) of the implant. A typical gaussian distribution as predicted by the LSS theory is shown in Figure 2.

9

Figure 1.   Definition of Range R and Projected
Range R_p

$$N_p = \frac{\phi}{\sqrt{2\pi}\Delta R_p}$$

ϕ = Ion Dose (cm^{-2})

$$N(x)=N_p \ exp\left[-\frac{(x-R_p)^2}{2\Delta R_p^2}\right]$$

NORMALIZED CONCENTRATION

R_p

ΔR_p

Background
Concentration

DISTANCE

Figure 2. Typical LSS Gaussian Distribution

11

III Glow Discharge Optical Spectroscopy

Discharges

When two electrodes are placed in an evacuated chamber
containing argon or any of the inert gases, and a suf-
ficiently large field is applied across the terminals, a
self-sustaining dc discharge is produced (Ref 5:125-140).
This discharge is characterized by light and dark regions
as shown in Figure 3.

Using argon, a blue discharge is produced when argon
molecules are ionized and these ions strike the cathode,
emitting electrons. Electrons are also produced at the
cathode by photoionization from high-energy photons pro-
duced in the discharge. Electrons freed from the cathode
are accelerated toward the anode, colliding with gas
molecules as they travel. The electrons are unable to
produce a large number of ionizations until they have gained
sufficient energy. This explains the dark space immedi-
ately next to the cathode (called Aston's dark space). The
luminous region outside the dark space is called the cathode
glow region. In this region the gas molecules have acquired
sufficient energy to produce light after colliding with
other molecules.

Because most of the electrons have undergone a number
of excitation collisions, they now have small velocities
and can produce neither ions nor photons, thus this region
is dark (called the cathode dark space). Emitted cathode

12

Aston's
Dark Space

Cathode
Dark Space

Faraday
Dark Space

Cathode
(-)

Anode
(+)

(a)

Cathode
Glow

Negative
Glow

Positive
Column

Cathode
Fall

(b)

Luminous Intensity

Figure 3. (a) Distinct Regions of D.C.Discharge
(b) Luminous Intensity
(From Ref 5:126)

13

electrons which have accelerated beyond the cathode glow region without experiencing any collisions now have enough energy to ionize the gas. However, this ionization produces electrons which do not have sufficient energy to excite the gas molecules and thus contribute no light in the cathode dark space. The electrons from the cathode dark space are now accelerated by the electric field until they have sufficient energy to produce light due to excitation collisions. This region is called the negative glow region.

The Faraday dark space results from the fact that the electrons from the negative glow region lack sufficient energy to ionize the gas. After accelerating out of this dark space electrons produce light in the positive column region. The momentum of these electrons is much greater than the momentum of the positive gas ions in this region thus there is little or no chance of recombination.

The region near the cathode is the area of interest in GDOS. The region consisting of Aston's dark space, the cathode glow, and the cathode dark space is called the cathode fall region. The size of the cathode fall is a function of cathode material and inert gas used. In a normal glow discharge the current density and the cathode fall voltage are held constant and the cathode glow does not cover the entire cathode.

However, most sputtering is done in the abnormal glow region. The entire cathode is covered by the glow and

14

with increasing current, the current density increases. In contrast to the normal glow, the cathode fall voltage is no longer constant, but is a function of pressure and current density (Ref 6:226-227).

Sputtering

Sputter etching is the process of removing the surface of a material by continual bombardment of the surface by ions. Sputtering is a function of many variables including the masses of the ion and the target atom, the ion energy, the direction of incidence to the face of the target, and the ion flux (current density). Measured sputtering yield also depends on the background gas pressure, concentration of implanted ions, and electric field at the surface of the target (Ref 7:111-128).

The prediction of sputtering yield is quite complex but good results have been obtained by the theories of Thompson and Sigmund (Ref 7:115-125). The exact sequence of events in sputtering is still disputed, but it is commonly agreed that many target atoms are sputtered per incident ion. It has been observed that for a crystalline solid atoms are ejected along the close packing directions of the material. For a diamond lattice like silicon atoms are ejected preferentially along the (111) and (100) directions (Ref 10). In GDOS, physical sputtering as described above is used. Reactive sputtering, due to chemical reaction between the gas and the cathode, can be neglected because

15

such a reaction is minimal in a low pressure inert gas atmosphere.

When sputtered, most of the ejected particles are in an electrically neutral state (Ref 8). Any ionized atom in the cathode fall region would be accelerated back toward the cathode. Research has shown that when GaAs is sputtered, the neutral atoms Ga and As are ejected, and these atoms are ejected stoichiometrically from the (111) face of GaAs (Ref 9).

Another factor to be considered when using sputtering is that sputtering is commonly used to deposit thin films of metals on substrates. To prevent contamination of the discharge, the sputtered atoms must stick to the walls of the chamber. The rate of deposition on the walls is a function of pressure, and the number of collisions for a sputtered atom increases with pressure. In GDOS, the chamber pressure must be kept low because at higher pressures the sputtered atoms may be reflected back toward the cathode.

GDOS

Light from a glow discharge contains emission lines corresponding to the atomic species of cathode material. The sputtered atoms are excited in the discharge and give off light. It can be shown that the intensity of the emission is proportional to the concentration of impurity atoms (Ref 11:13-16). The constants of proportionality

16

are in fact very difficult to calculate. However, by carefully keeping the discharge constant, calibration with a pure substance can be accomplished.

The GDOS technique has been shown to be effective as an analytical depth profiling technique (Ref 12). In principal any element can be analyzed with GDOS. In practice, however, it is found that the emission lines of some elements are much better suited to analysis than those of other elements.

IV   Experimental Apparatus

A plan view of the GDOS system used in these experi-
ments is shown in Figure 4. For descriptive purposes the
equipment is classified into the following categories:

1. Sputtering chamber assembly

2. Vacuum, gas, and cooling systems

3. Detection and recording systems

Sputtering Chamber Assembly

The heart of the GDOS system is the sputtering chamber
shown in Figure 5. The chamber was made from a 3" diameter,
6" high pyrex glass cylinder with three open ports, each
extending 4-1/2" from the center. The port openings were
covered with silica quartz windows to allow ultraviolet
light transmission. The substrate monitor window was 2"
in diameter and 1/8" thick. Located at right angles to
this window are the two 2-3/4" diameter windows used for
light collection in the impurity detection system. Very
little material is deposited on the windows because they
are mounted perpendicular to the sample. The light collec-
tion efficiency of the impurity detection system was im-
proved by a 3" diameter spherical mirror placed directly
opposite the 2-1/4" diameter collecting lens.

The chamber is sealed with 1/8" thick rubber gaskets
which are countersunk in grooves and by 1/2" thick stainless
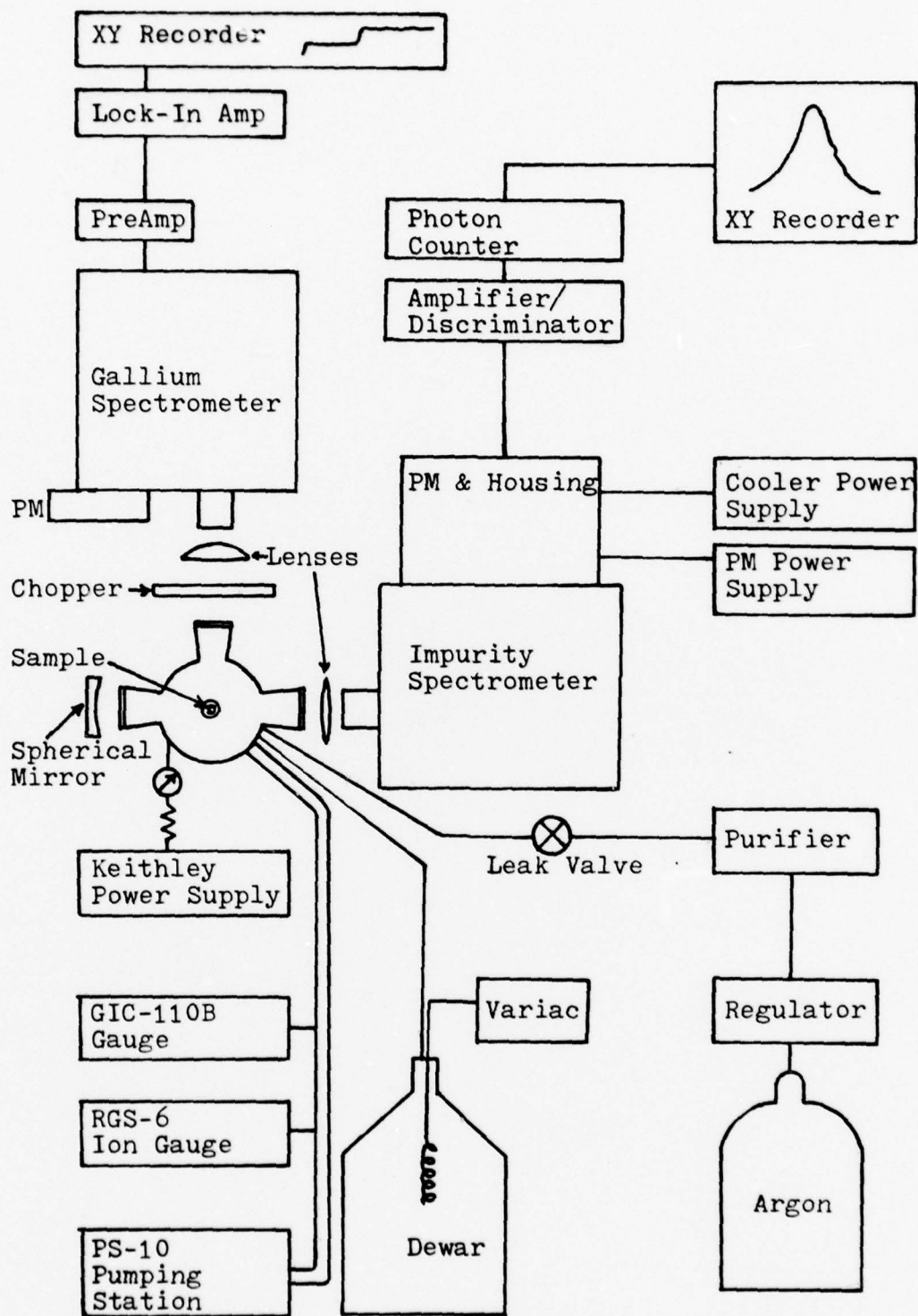steel top and bottom plates. The top plate is at ground
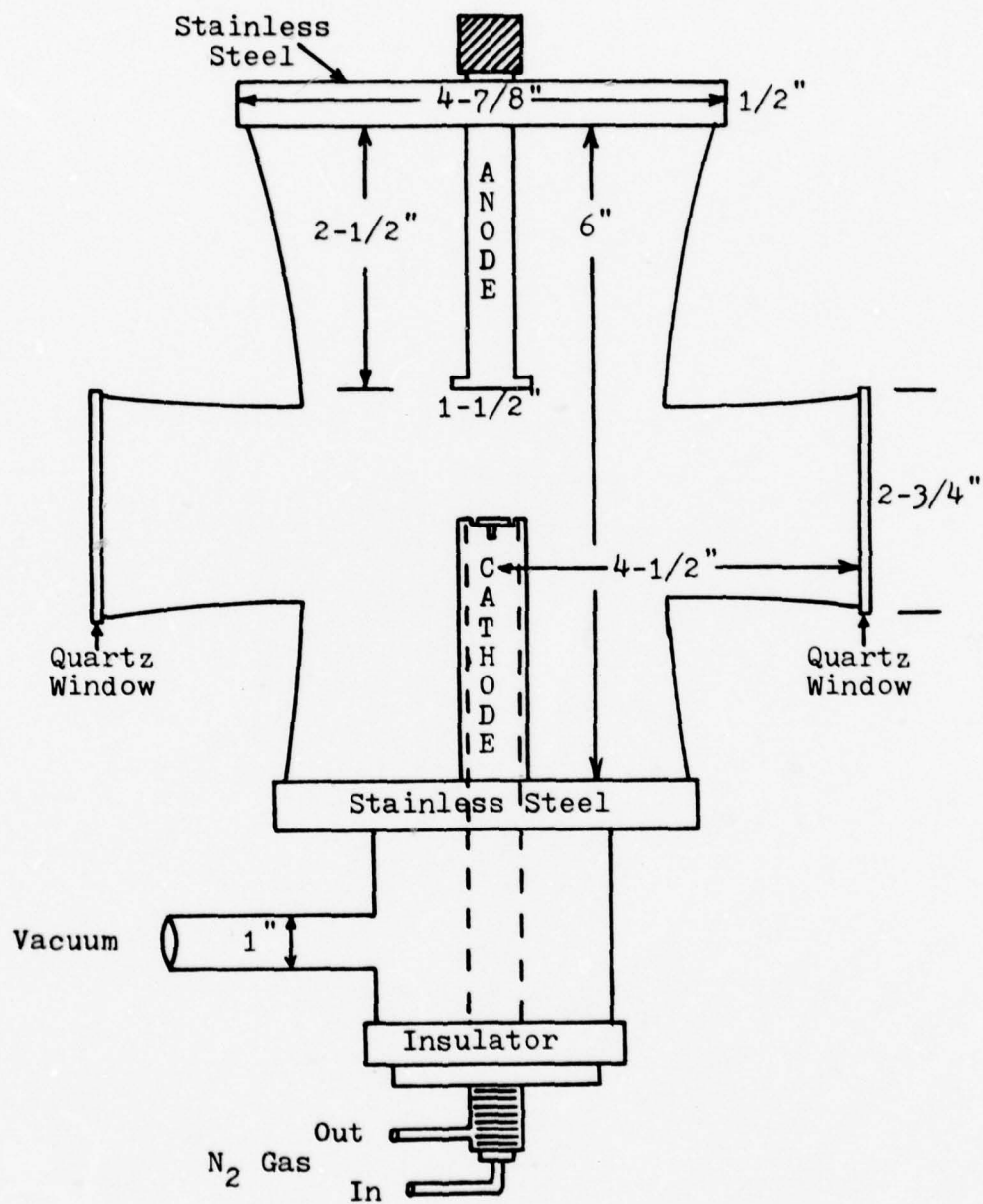
18

Figure 4.   Plan View of GDOS Apparatus

19

Figure 5. Sputtering Chamber

20

potential and has a 1" diameter, 2-1/2" long shaft with
a 1-1/2"diameter cylindrical stub forming the anode. The
bottom plate is also at ground potential and the cathode
electrode is a 3/4" diameter hollow copper shaft insulated
from the plate by teflon washers. This hollow electrode is
fitted with inlet and outlet tubes for circulation of
cooling nitrogen gas. The cathode is constructed by ce-
menting a 1/2" diameter circular tungsten plate on a
machined aluminum cap with a small 1/2" diameter circular
step. The cathode to anode separation is 1". The entire
lower electrode, with the exception of the tungsten cathode,
is protected with a closely fitting pyrex glass shield.
A diagram of the cathode configuration is shown in Figure 6.
The lower electrode assembly is also fitted with a vacuum
port and a thermocouple gauge.

The cathode electrode is connected to the negative
high voltage source. The negative voltage was supplied
by a Keithley Instruments Model 242 Regulated High Voltage
Supply, with a range of ±3500 volts at 25 milliamps. A
160 Kohm resistor network was used between the supply and
the cathode electrode to limit the ion current and protect
the power supply from accidental short-circuits. Also
connected in this circuit was a dc milliameter used to
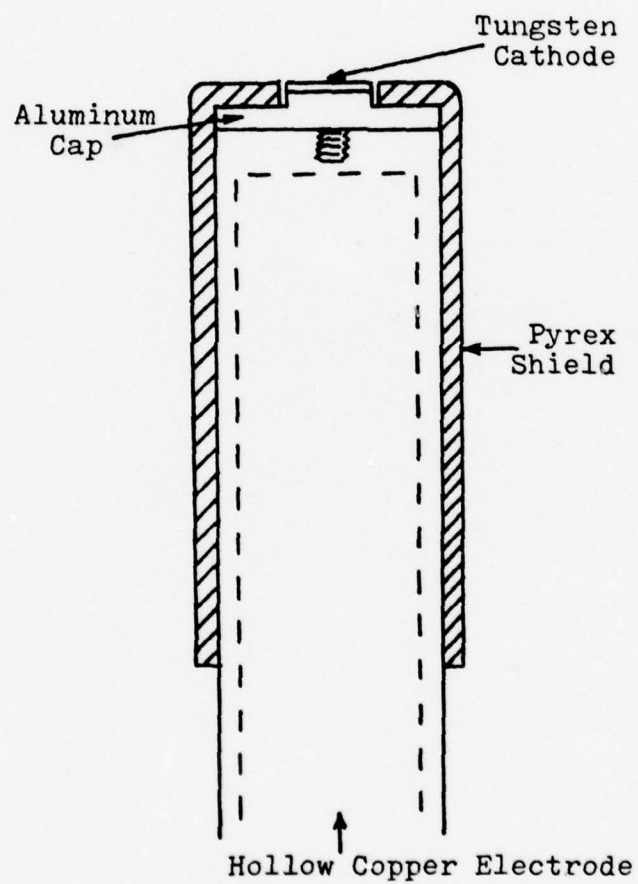monitor the ion current.

21

Figure 6. Cathode Configuration

Vacuum, Gas, and Cooling System

Evacuation of the sputtering chamber was done with
a Varian Model PS-10 Pumping Station. The PS-10 has a
single mechanical pump for roughing and for backing of the
diffusion pump, and an oil diffusion pump with a liquid
nitrogen cooled cold trap for high vacuum. High vacuum
was measured with a Veeco Instruments RGS-6 Ionization
Gauge Control with a RG75P ion gauge. Medium vacuum was
measured with a Consolidated Vacuum Corporation Model
GIC-110B Ionization Vacuum Gauge connected to a thermo-
couple mounted on the cathode assembly.

Regulated argon gas was supplied to the chamber through
a Hydrox Purifier Model 8301. Gas purity was approximately
99.9 percent. Gas flow to the chamber was controlled with
a leak valve manufactured by Granville-Phillips Co.

Nitrogen gas for cooling the lower electrode was
provided by a ten liter Dewar container. A heating element
submersed in the liquid nitrogen was controlled by a Variac
autotransformer. The gas was piped through a teflon tube
to the lower electrode assembly.

Detection and Recording Systems

The detection system actually consisted of two indepen-
dent systems. One system was used to monitor the impurity
line of interest. The other system was used to monitor
gallium in the substrate.

For the impurity line, light gathered by the 2-1/4" diameter plano-convex quartz lens was focused on the entrance slit of a Spex Industries Model 1704 one-meter Czerny-Turner Scanning Spectrometer. A Bausch and Lomb diffraction grating ruled with 1200 lines/mm and blazed at 3000 Å was mounted on the spectrometer. The variable entrance and exit slits were set at 200 and 400 microns respectively and the spectrometer was used in the mono-chromatic mode.

The output at the spectrometer exit slit was detected with an RCA C31034 eleven-stage Quantacon photomultiplier tube. The tube had a 2" ultraviolet transmitting window and a GaAs photocathode. The typical amplification of the tube is 6×10^5 when cooled. A PAR Model TE-104 thermo-electrically refrigerated chamber was used to cool the tube. It was capable of cooling the tube to below -20°C. After cooling the tube for approximately two hours, the dark count was maintained below 20 counts per second. Bias for the multiplier tube was supplied by a Fluke Model 412B dc High Voltage Power Supply set at -1760 volts.

The photomultiplier output was fed to an SSR Instruments Co. Model 1120 Amplifier/Discriminator and to a Model 1108 Multi-Mode Processor Photon Counter. This counting system allows for count times from one microsecond to 1000 seconds, with a pulse pair resolution of 12 nano-seconds, and a maximum signal rate of 85 megahertz.

24

The normal mode of operation for the experiments was a one second preset counting time.

The logarithmic voltage output of the photon counter, (proportional to photon counts), was displayed on the Y-axis of a Hewlett-Packard 7004B Recorder. The Y-axis sensitivities ranged from 0.5 millivolts to 10 volts/inch. The X-axis represented sputtering time, and scan speeds ranged from 0.5 to 100 sec/inch.

For the gallium line, light gathered by the 3-1/2" diameter convex quartz lens was chopped by a PAR Model 191 variable speed chopper. The light was then focused on the entrance slit of a Spex Industries Model 1799-II 3/4 meter Czerny-Turner spectrometer. A Bausch and Lomb diffraction grating ruled with 1000 lines/mm and blazed at 3000 $\overset{\mathrm{o}}{\mathrm{A}}$ was mounted on the spectrometer. The variable entrance and exit slits were set at 100 and 200 microns respectively and the spectrometer was used in the mono-chromatic mode.

The output at the spectrometer exit slit was detected with a Spex Model 1424 photomultiplier. The photomultiplier output was fed to PAR Models 221 and 116 pre-amplifiers and then to a PAR Model 124A Lock-In Amplifier. The lock-in amplifier was capable of accurate signal measurements from 100 picovolts to 5000 millivolts at frequencies from 0.2 Hz to 210 kHz. The signal from the lock-in amplifier was recorded on the Y-axis of a Houston Instrument Omnigraphic 3000 XY Recorder. The Y-axis sensitivities ranged from

25

1 to 2000 millivolts/inch. The X-axis of the recorder
represents sputtering time and scan speeds ranged from
0.05 to 20 inches/min.

V   Experimental Procedure

Sample Preparation

The samples used in this study were cut from wafers of melt grown, undoped GaAs substrate prepared by the Laser Diode Laboratories. Initial experiments with Ge and Mg implants were carried out with square samples 0.5 cm on a side. Final experiments with boron were conducted with square samples cut 0.75 cm on a side. The increased surface area produced greater intensity distributions and eliminated the need for perimeter chips which were necessary with smaller samples. The perimeter chips, shown in Figure 8, were cut from undoped GaAs substrate material and were 0.125 cm by 0.625 cm. By using these chips with the smaller samples, uniform surface sputtering of the samples could be obtained because sharp edges, which cause high local current densities and strong electric fields near them, leading to increased sputtering at the edges, were eliminated.

Preliminary samples were first etched in a dilute H_2SO_4/H_2O_2 solution before implantation; however, it was soon discovered that this etching produced uneven surfaces and therefore non-uniform sputtering of the surface. Subsequent samples, including all samples described in this report were not etched before implantation but were prepared using a standard cleaning procedure used by Air Force Avionics Laboratory personnel.

27

Ion implantation of the sample was done in the
Air Force Avionics Laboratories Research Branch, AFAL/DHR,
with a highly modified accelerator manufactured by Accel-
erators, Inc. of Austin, Texas. The accelerator has a
maximum implant energy of 120 keV. All samples were im-
planted at room temperatures and were mounted at approx-
imately 7° from the normal to avoid channeling effects. All
samples were also from (100) oriented substrate. Germanium
ions were implanted at 120 keV at a fluence of 10^{15}ions/cm^2.
Magnesium ions were implanted at 60 and 120 keV at a fluence
of 5×10^{15} ions/cm^2. Boron ions were implanted at 60 and
120 keV at a fluence of 10^{15}ions/cm^2. Some boron samples
were multiply implanted at 60 and 120 keV at a fluence of
10^{15} ions/cm^2.

After implantation most of the samples were capped with
a 1000$\overset{o}{A}$ layer of Si_3N_4 to allow stabilazation of the dis-
charge before the implanted substrate was sputtered. The
Si_3N_4 cap was applied using two different methods. The
first method, which is most commonly used in the AFAL/DHR
Laboratory is the pyrolytic cap. This cap requires that the
sample be heated to approximately 700^oC in an atmosphere of
silane and nitrogen. The second method which is presently
in the experimental stage is the plasma enhanced cap. In
this method the sample is placed in a plasma of silane and
nitrogen. The temperature of the plasma is approximately
400° and the significance of the temperature difference be-
tween the two methods is discussed in Chapter VII.

Sputtering Rate Determination

In order to accurately profile an implanted sample the sputtering rate first had to be determined. By placing two small squares of GaAs on opposite sides of the sample being profiled and sputtering all pieces simultaneously in the discharge chamber, a step in thickness from etched to un-etched regions of the sample is produced and the sputtering rate can be calculated with the use of a Dektak Measuring System. A Sloan Dektak Surface Measuring System consisting of the Dektak and associated chart recorder was used to measure the height of the step after sputtering (Figure 7). The Dektak was capable of measuring step heights from 25 to 1,000,000 $\overset{o}{A}$. Sputtering rates were determined for samples of unimplanted GaAs and also for samples implanted with ger-manium, magnesium, and boron. Sputtering rates were also determined for both the pyrolytic and plasma Si_3N_4 caps. The results of these are given in Chapter VI.

GDOS System Operation

After placing the sample to be sputtered in the discharge chamber, the chamber was evacuated to approximately 2×10^{-5} torr to reduce contaminants. During the evacuation the cathode was cooled with nitrogen gas from the Dewar con-tainer. The chamber was then backfilled with high-purity (99.99 per cent) argon gas and a constant flow of gas was maintained by a leak valve. Pressure in the chamber was allowed to stabilize and was maintained at $25 \pm \frac{1}{2}$ micron.
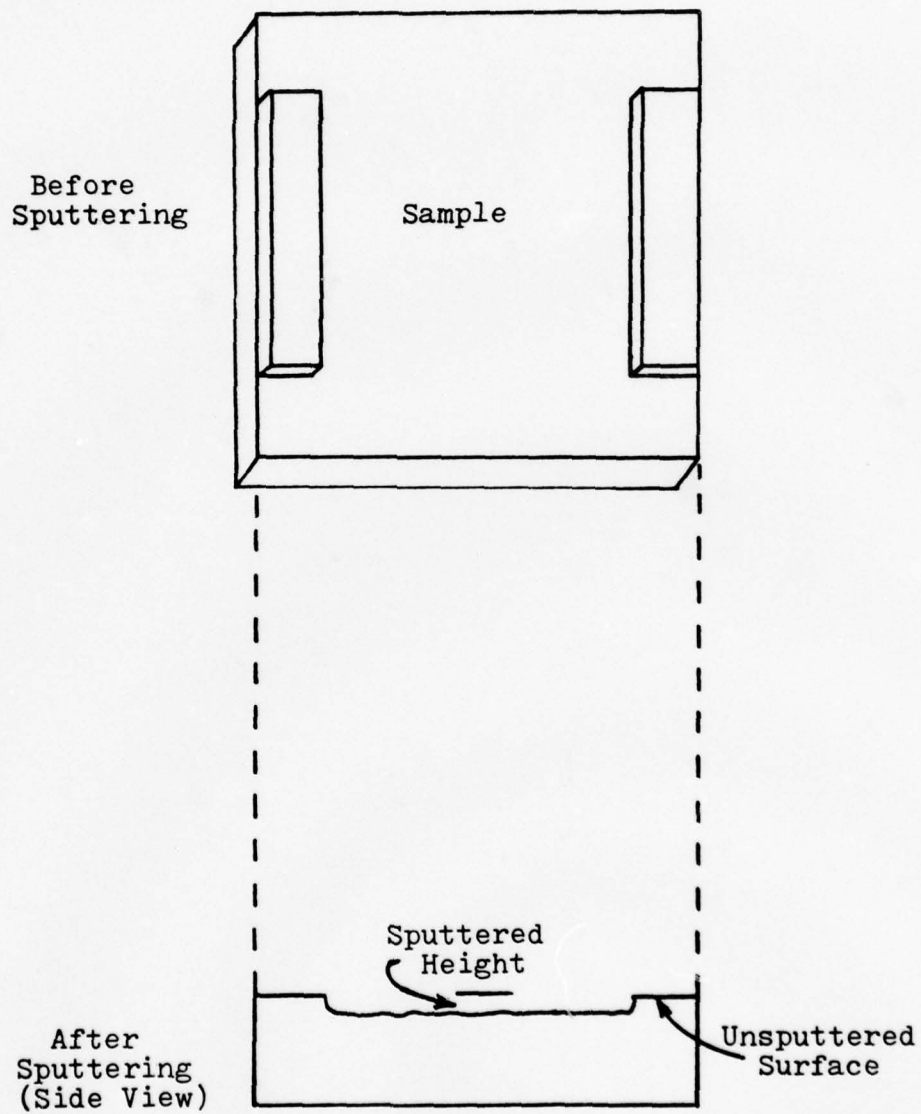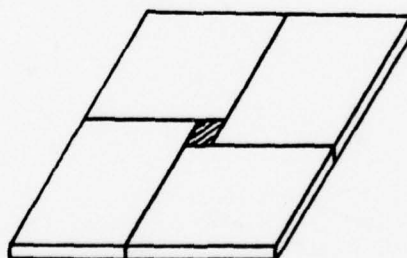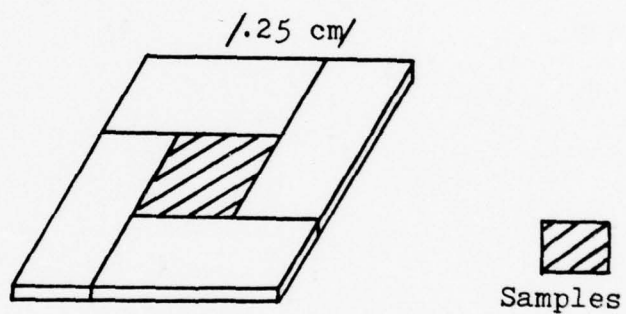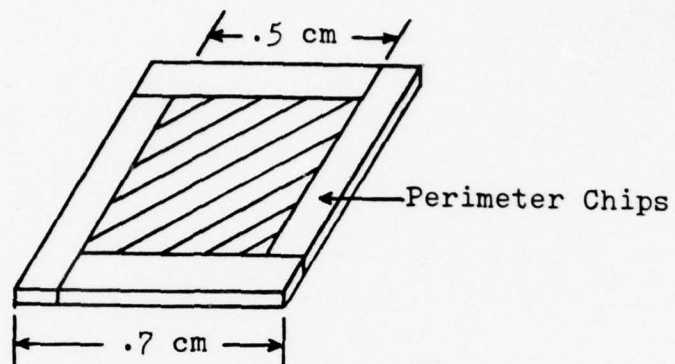
29

Figure 7. Sputtering Rate Determination

30

Figure 8. Calibration Sample Geometries

31

After the recorders were turned on the discharge was started by applying a 2100 volt potential across the electrodes. After the discharge is started, a short time, ranging from seconds to tens of seconds, is required to attain a steady-state sputtering condition. During this time surface oxides and contaminants are removed (Ref 13:618). The effect of this transition period on shallow and deep implants is discussed in Chapter VI.

GDOS System Calibration

In order for the GDOS intensity profile to be quantitetively meaningful, the system must first be calibrated. Unfortunately, bulk doped GaAs containing germanium, magnesium, or boron is not available to date. An attempt was made to calibrate the system using samples of pure germanium, magnesium and boron. By calculating the densities of the pure elements and then observing the intensity of spectral lines while sputtering samples of known size, the concentrations of the various implanted samples can be determined by linearly relating the two results. This linear relationship is predicated on the assumption that implanted impurity atoms ionize as readily as atoms of the pure element. This assumption was experimentally shown to be valid for germanium, magnesium, and boron as discussed in the next chapter.

VI Results and Discussion

Calibration Results

For purposes of sputter rate determination, a "standard" pressure and potential had first to be established. After sputtering many samples at different chamber partial pressures and voltages, it was determined that the best sputtering could be obtained at a chamber partial pressure of 25 microns with a voltage of 2100 volts. This combination of pressure and voltage was used for all experiments described in this thesis.

By using the step height recording procedure discussed in Chapter V, the sputtering rate of unimplanted GaAs was determined to be 1150Å/min. Measured sputtering rates for samples implanted with germanium, magnesium, and boron were within two percent of this figure and therefore a sputtering rate of 1150Å/min was used for depth determination in all experiments. Similarly, the sputtering rate for Si_3N_4 was determined to be 625Å/min.

In order to relate the intensity of sputtered Ge to actual concentration, the density (in atoms/cc) was first calculated to be 4.417×10^{22} atoms/cc in the following manner:

$$\frac{1}{72.59 \text{AMU}} \quad \frac{1 \text{AMU}}{1.659 \times 10^{-24} \text{gm}} \quad \frac{5.323 \text{gm}}{\text{cc}} = 4.417 \times 10^{22} \text{ atoms/cc}$$

33

By observing a photon count of 44,000 per second while sputtering the Ge sample, a linear proportionality constant between observed intensity (in photon counts) and concentration was calculated for Ge from:

$$4.417 \times 10^{22} \text{atoms/cc} \quad \frac{1}{44,000 \text{ counts}} = 1 \times 10^{18} \text{atoms/cc/count}$$

In order to determine if the relationship between observed intensity and concentration is truly linear, sputtered sample sizes of pure germanium were sucessively decreased. When the sample size was decreased to $1/4^{\text{th}}$ the original size (0.25 cm square), the observed photon count was also reduced by approximately $1/4^{\text{th}}$ to 11,050. As shown in Figure 8 perimeter chips were successively increased in size to preserve the original geometry and keep the total sputtering rate constant. For the smallest geometry of Ge used ($1/64^{\text{th}}$ of the original size), the observed photon count was also reduced by approximately $1/64^{\text{th}}$ to 700, showing that the relationship is truly linear.

The density of pure magnesium was calculated to be 4.312×10^{22} atoms/cc from:

$$\frac{1}{24.312 \text{AMU}} \quad \frac{1 \text{AMU}}{1.659 \times 10^{-24} \text{gm}} \quad \frac{1.74 \text{gm}}{\text{cc}} = 4.312 \times 10^{22} \text{ atoms/cc}$$

By observing a photon count of 423,000 per second while sputtering a pure magnesium sample, a linear relationship

between observed intensity and concentration was calculated for Mg to be:

$$4.312 \times 10^{22} \text{atoms/cc} \quad \frac{1}{423,000 \text{ counts}} = 1.019 \times 10^{17} \text{atoms/cc/count}$$

Similarly, the density of pure boron was calculated to be 1.304×10^{23} atoms/cc from:

$$\frac{1}{10.811 \text{AMU}} \quad \frac{1 \text{AMU}}{1.659 \times 10^{-24} \text{gm}} \quad \frac{2.34 \text{gm}}{\text{cc}} = 1.304 \times 10^{23} \text{ atoms/cc}$$

As mentioned in Chapter V, the size of the boron samples was doubled to 0.75 cm squares to improve the intensity distribution and eliminate the need for perimeter chips. For this reason, a 0.75 cm square was also used for calibration of the boron source. Also, the sensitivity of the impurity measuring system was greatly improved by replacing the RCA Quantacon photomultiplier tube with a new one. After calculating a photon count of 1.19×10^7/ sec by using a smaller pure boron sample, the proportionality factor between the observed intensity and concentration was calculated for boron to be:

$$1.304 \times 10^{23} \text{atoms/cc} \quad \frac{1}{1.19 \times 10^7 \text{counts}} = 1.09 \times 10^{16} \text{atoms/cc/count}$$

Germanium Implants

The profile obtained for an as-implanted Ge sample is shown in Figure 9. The sample was capped with a 1000Å Si_3N_4 plasma cap. The measured projected range of 500Å agrees favorably with the LSS calculated range of 476Å (Ref 14).

35

Ge Implanted GaAs
120keV, $\phi = 10^{15}cm^{-2}$
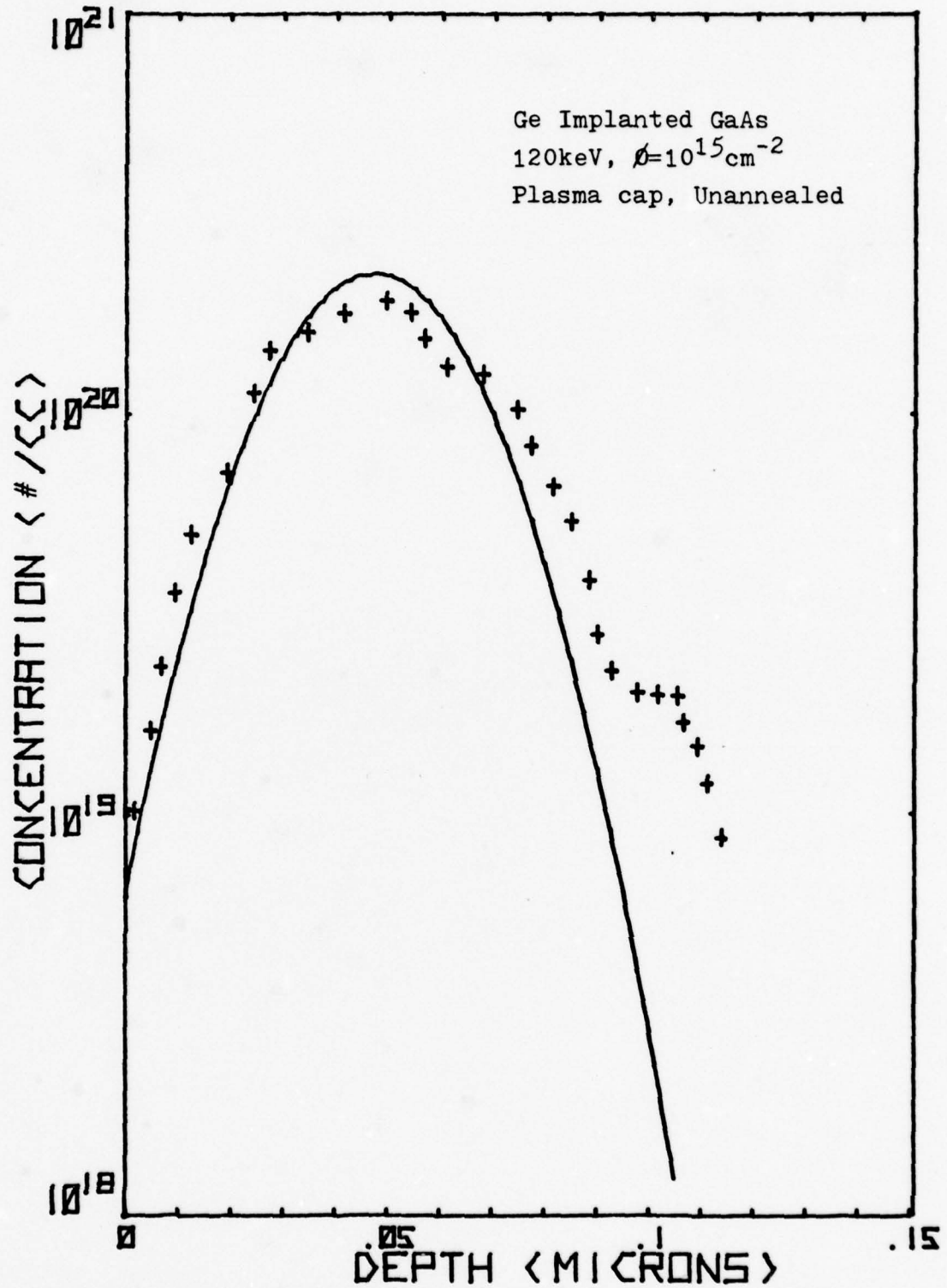Plasma cap, Unannealed

Figure 9.   Measured Profile of Ge Implanted GaAs
Compared to Theoretical LSS Profile

36

The slight difference may be due to the uncertainty of the exact location of the cap-surface interface. By monitoring the 4172.1Å gallium line and noting a sudden increase in the gallium intensity, the location of the cap-surface can be obtained as shown in Figure 10. Also, the sputtering rate of gallium as measured by the substrate monitor was uniform within five percent throughout the measurment. There is, of course, a simultaneous increase in germanium intensity due to surface concentration as monitored by the impurity spectrometer. The measured peak concentration of $1.9 \times 10^{20}/cm^3$ also compares favorably with the LSS predicted peak of $2.2 \times 10^{20}/cm^3$.

The measured profile for a second as-implanted Ge sample is shown in Figure 11. This sample was capped with a 1000Å Si_3N_4 pyrolytic cap. There is, however, no significant difference in the measured profiles between samples capped by the two different methods.

By increasing the sample size of an as-implanted Ge sample, an impurity profile was obtained for the sample without capping it (Figure 12). The measure projected range and peak concentration are in very close agreement with the predicted LSS values.

The measured profile for an annealed Ge-implanted sample is shown in Figure 13. The sample was capped with a 1000Å Si_3N_4 pyrolytic cap then annealed in flowing hydrogen gas for 15 min at $700^{\circ}C$. The measured projected range of 550Å
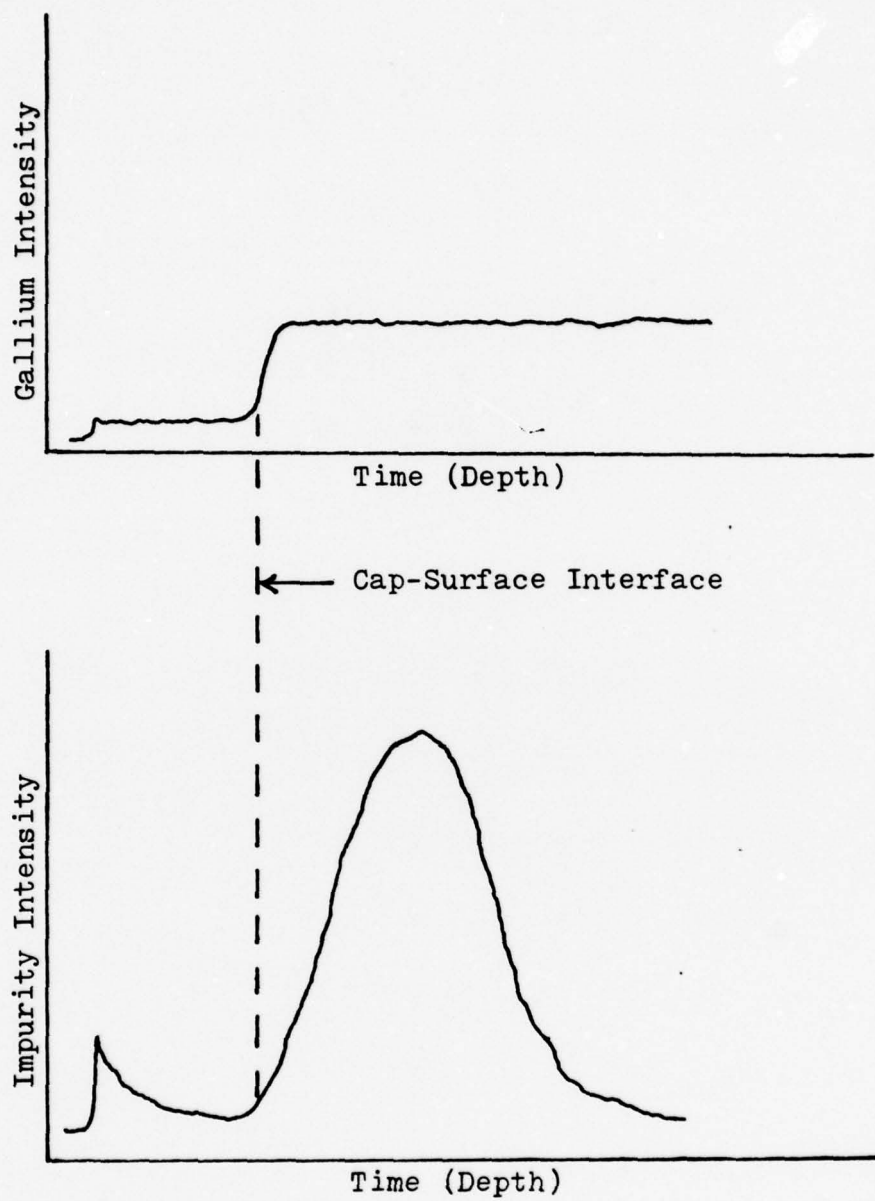
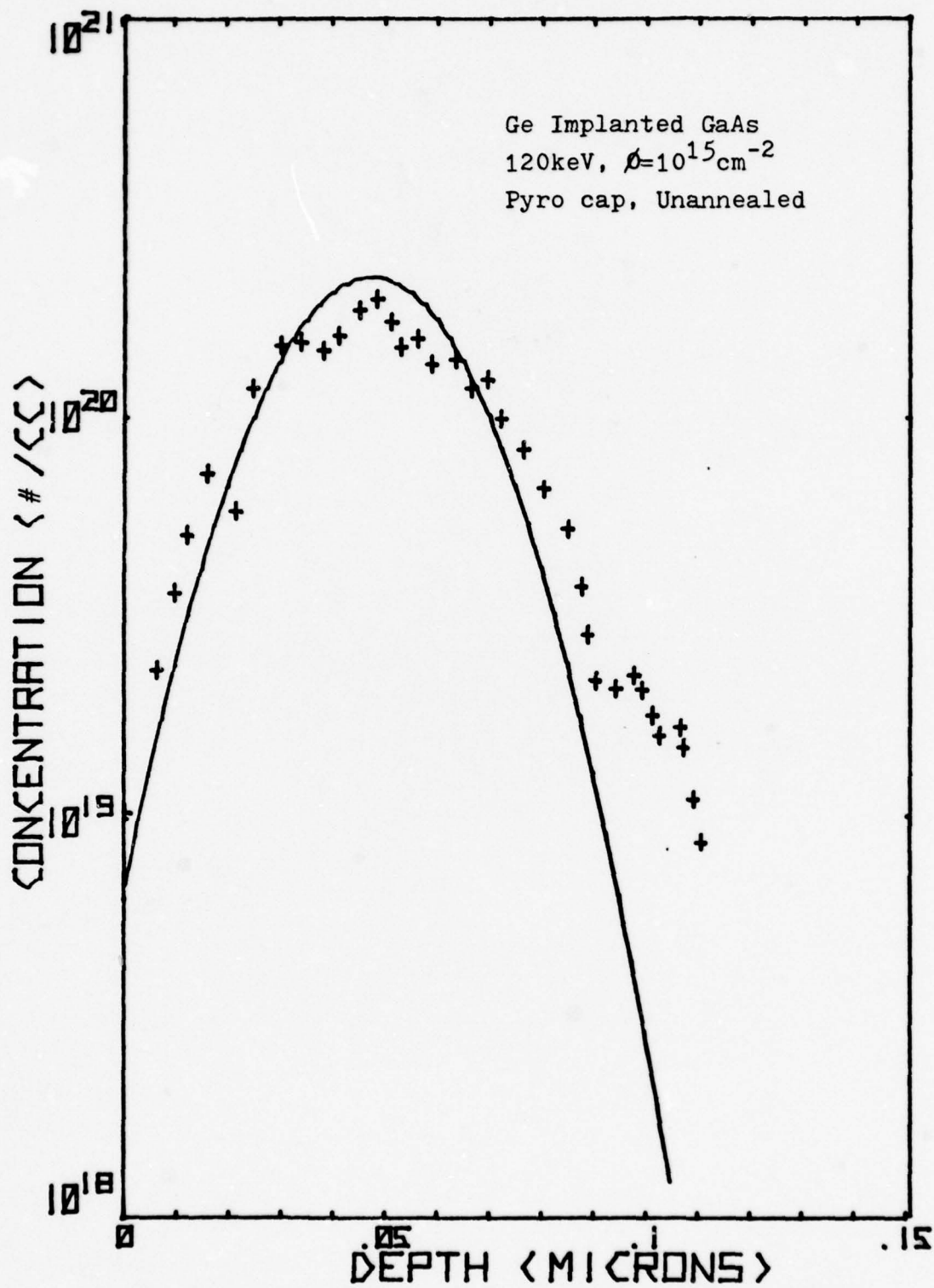Figure 10.   Determination of Cap-Surface Interface

38

Figure 11. Measured Profile of Ge Implanted GaAs
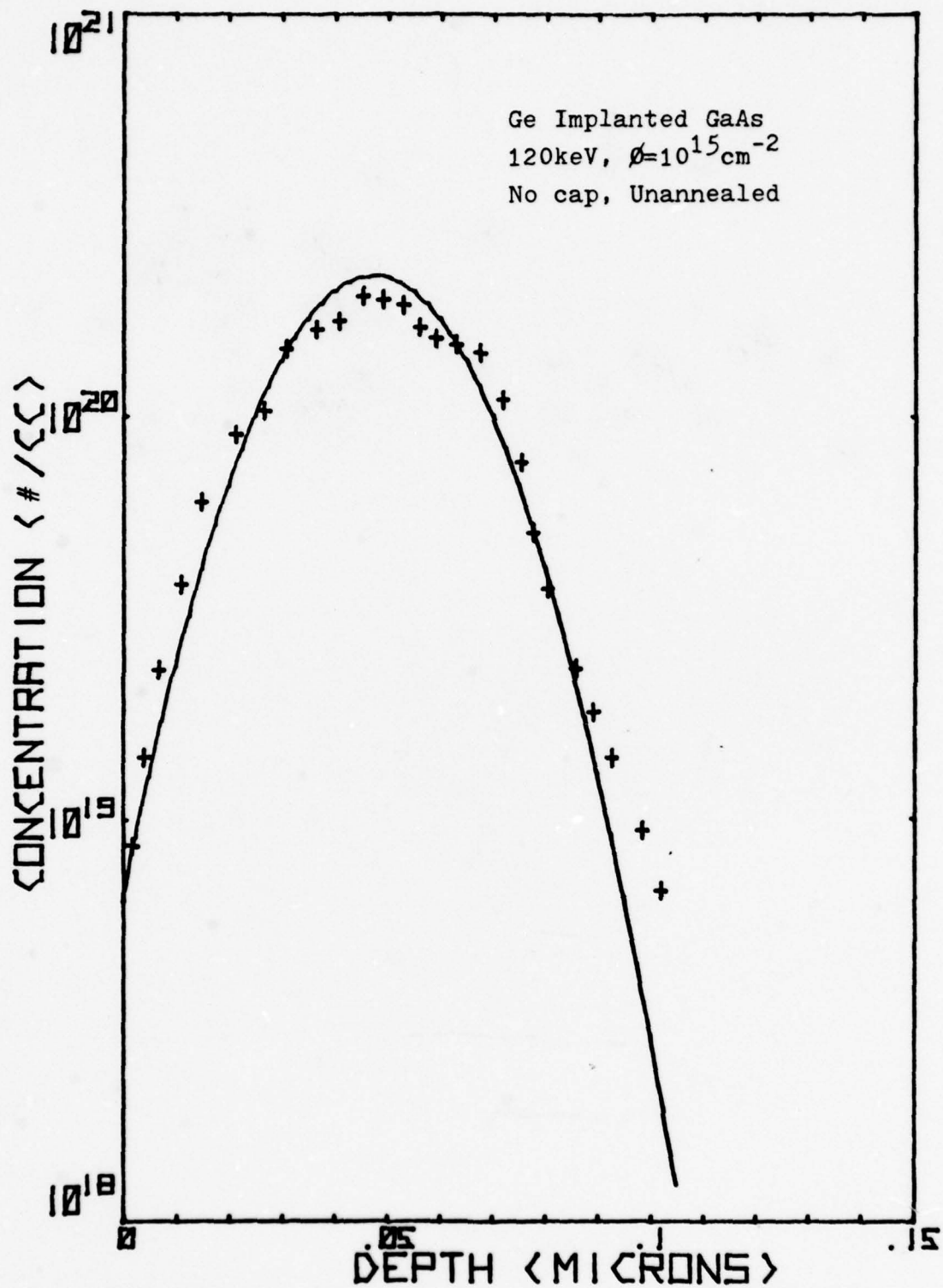Compared to Theoretical LSS Profile

Figure 12. Measured Profile of Ge Implanted GaAs
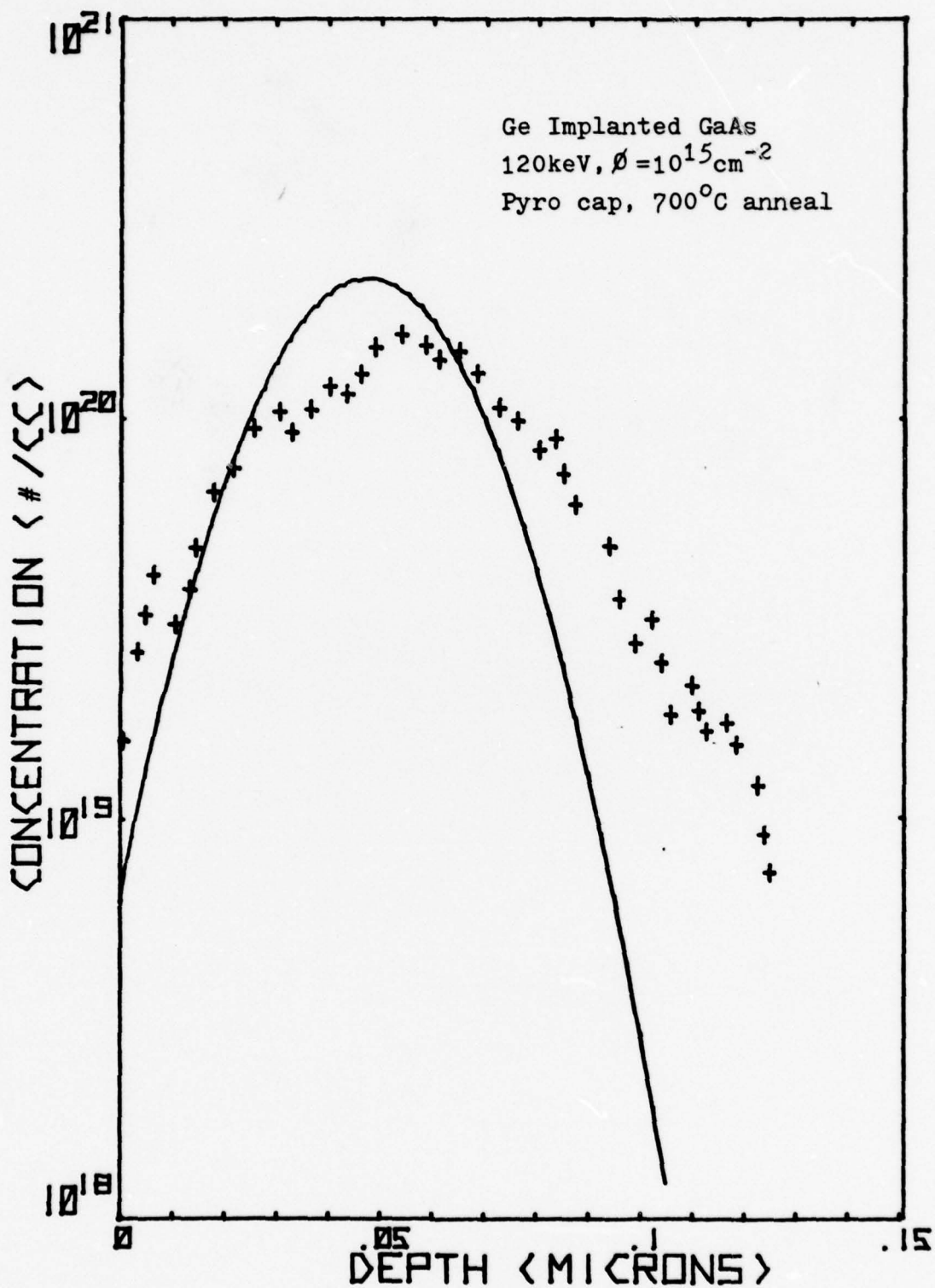Compared to Theoretical LSS Profile

Figure 13.   Measured Profile of Annealed Ge Implanted
GaAs Compared to Theoretical LSS Profile

41

is slightly greater than the LSS value of 476Å as expected.
The peak concentration is also noticeably lower than the LSS
prediction. These differences are due to the shifting of
the concentration profile toward the inside of the sample
due to diffusion. The effect of this shifting is minimal
for a 700°C anneal.

The effect of this shifting due to indiffusion is more
pronounced for a 900°C anneal, as shown in Figure 14. This
sample was also capped with a 1000Å Si_3N_4 pyrolytic cap.
The peak concentration is approximately $10^{20}/cm^3$ and is
located at 650Å. Also, the redistribution of implanted Ge
impurities extends to almost twice the width of the LSS
distribution.

Magnesium Implants

Impurity profiles were obtained for Mg-implanted
samples capped with pyrolytic and plasma Si_3N_4 caps. Very
different results were obtained with the two caps.

The profile obtained for an as-implanted Mg sample is
shown is Figure 15. The sample was capped with a 1000Å
Si_3N_4 plasma cap. The measure projected range of 1100Å is
slightly less than the LSS predicted range of 1230Å and this
may again be due to the cap-surface interface uncertainty.
Although the measured profile follows the LSS distribution,
a significant difference occurs between the measured and
peak concentration values. The measured peak is one and one-
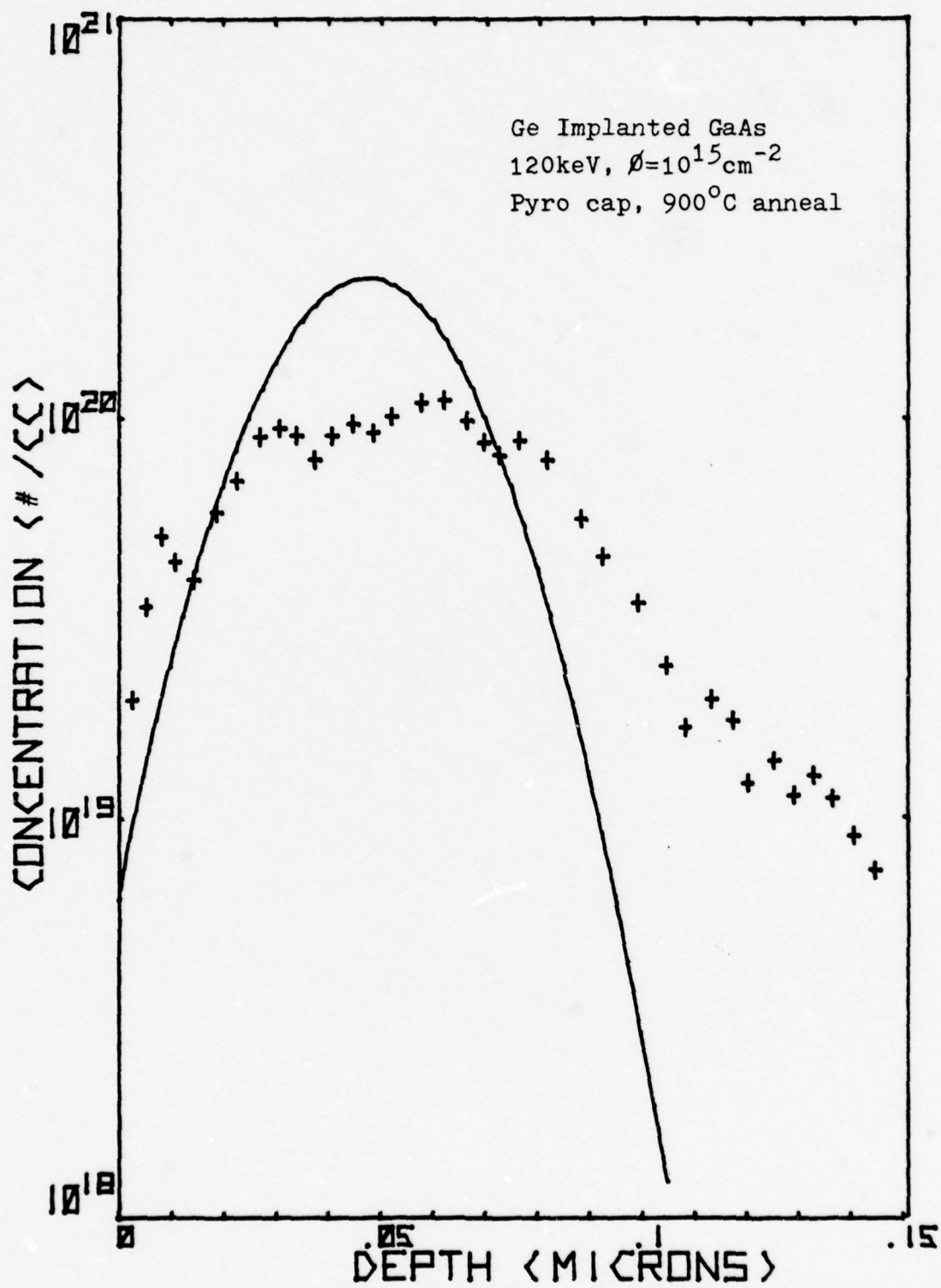half orders of magnitude lower than predicted peak. This

42

Figure 14. Measured Profile of Annealed Ge Implanted
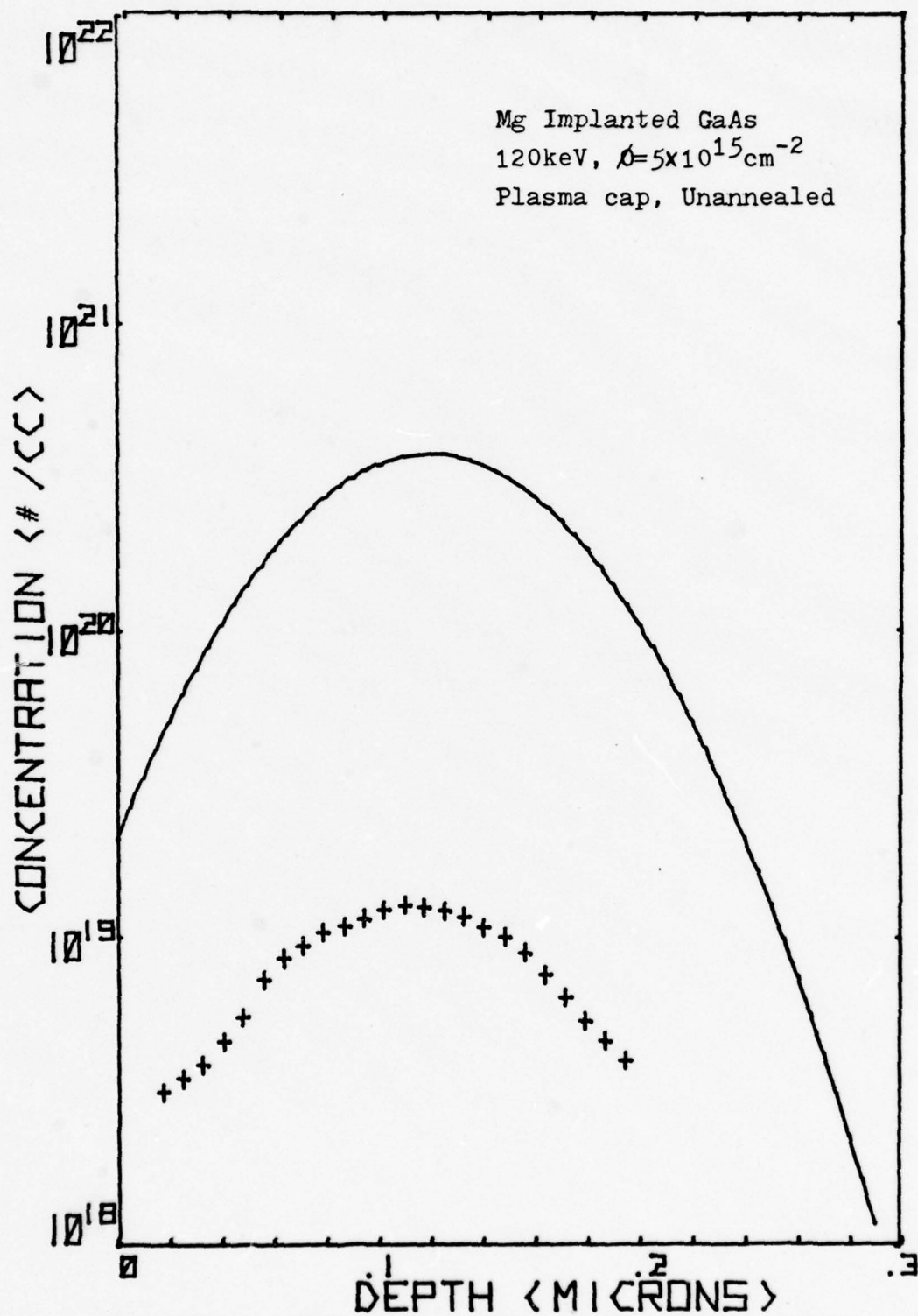GaAs Compared to Theoretical LSS Profile

43

Figure 15. Measured Profile of Mg Implanted GaAs Compared to Theoretical LSS Profile

difference may be due to several factors including outdiffusion during capping, solid-solubility limit for Mg in GaAs, or inaccurcy in the scale factor for measured intensity vs concentration. Outdiffusion during capping or annealing was the primary factor investigated in this thesis.

Annealing effects are aparrant in Figure 16. The sample was plasma capped and then annealed at 850°C for 15 min. The peak concentration is shifted to $1800\overset{\circ}{\text{A}}$ apparently due to indiffusion. The high surface concentration observed is apparently due to outdiffusion during the anneal.

A dramatic difference between plasma capped samples and pyrolytically capped samples is apparent in Figure 17. This figure shows an as-implanted Mg sample capped with a Si_3N_4 pyro cap. The large delta-like concentration of Mg at the surface is most probably due to outdiffusion (to and out of the surface) during capping. The secondary peak is again nearly coincident with the LSS predicted peak and its magnitude is again 1-1/2 orders of magnitude below the LSS calculated value.

In order to determine the annealing effects of pyrolytically capped Mg samples, two samples were annealed at 700°C and 900°C. Figure 18 shows a sample annealed at 700°C. A very large surface concentration indicates that more outdiffusion has taken place while the secondary peak shows no indiffusion whatsoever.

A 900°C annealed pyrolytically capped sample is shown

45

Figure 16. Measured Profile of Annealed Mg Implanted
GaAs Compared to Theoretical LSS Profile

46

CONCENTRATION (#/CC)

10^{22}

10^{21}

10^{20}

10^{19}

10^{18}

Mg Implanted GaAs
120keV, $\phi=5\times10^{15}$cm^{-2}
Pyro cap, Unannealed

0   .1   .2   .3
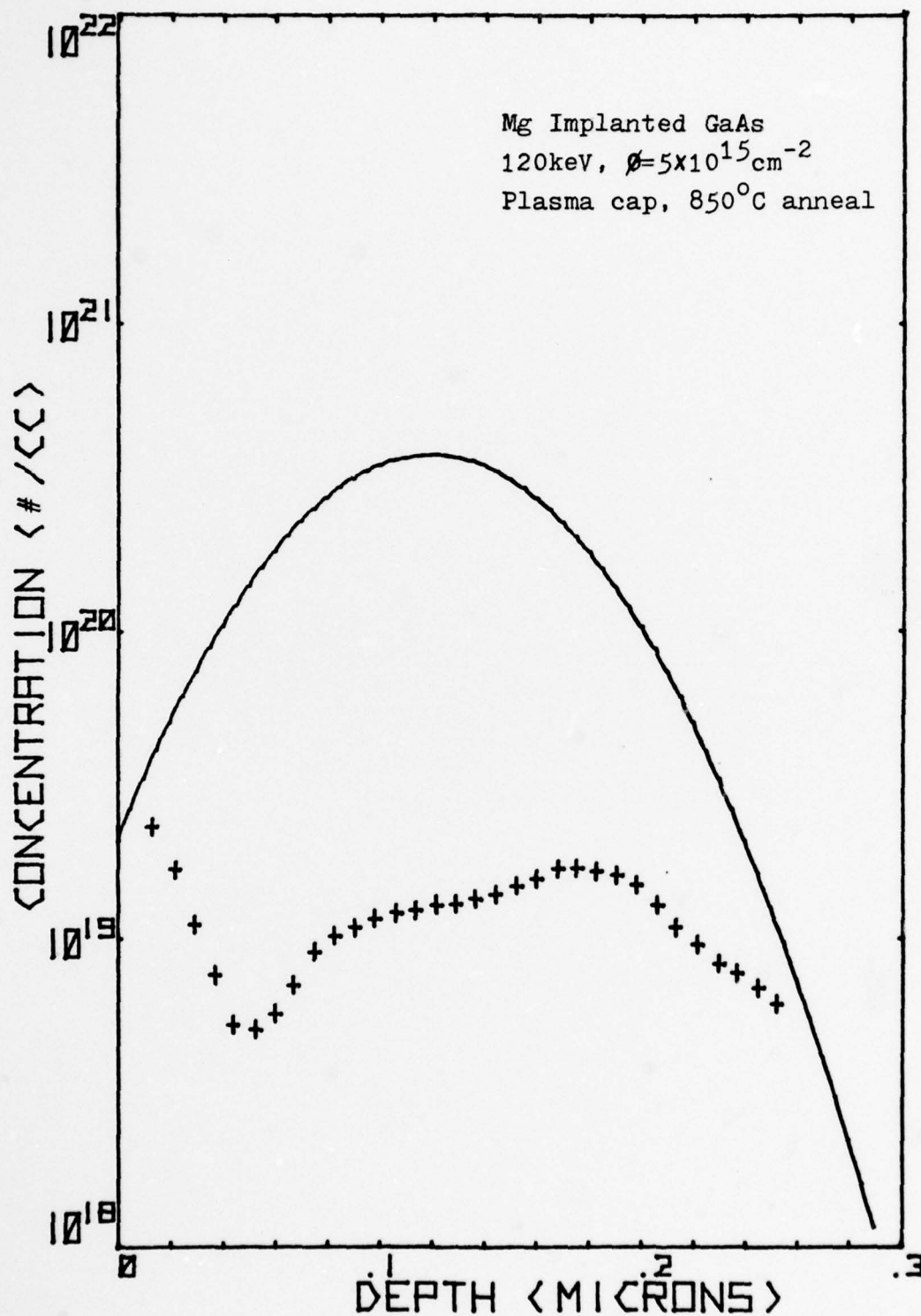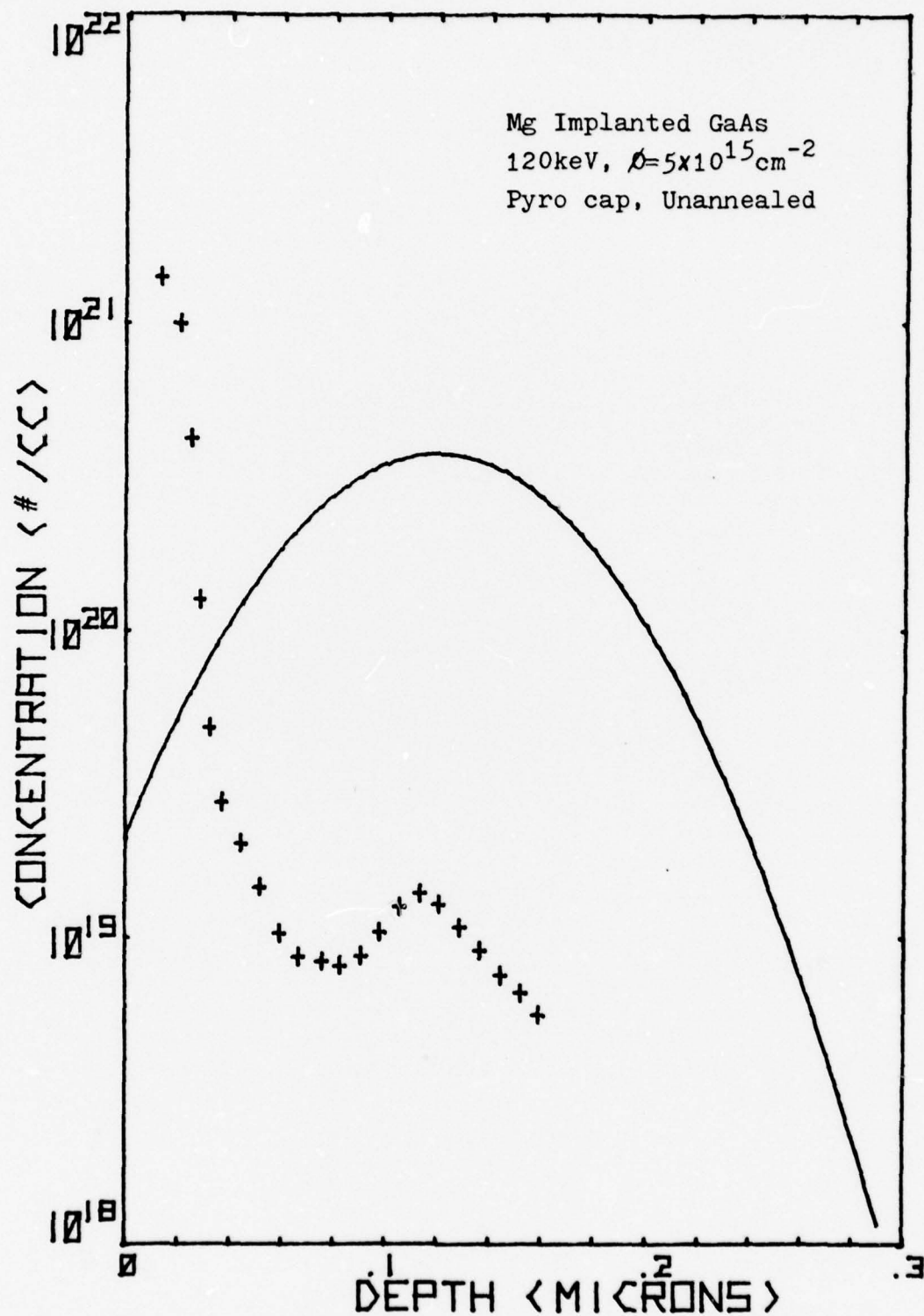
DEPTH (MICRONS)

Figure 17. Measured Profile of Mg Implanted GaAs
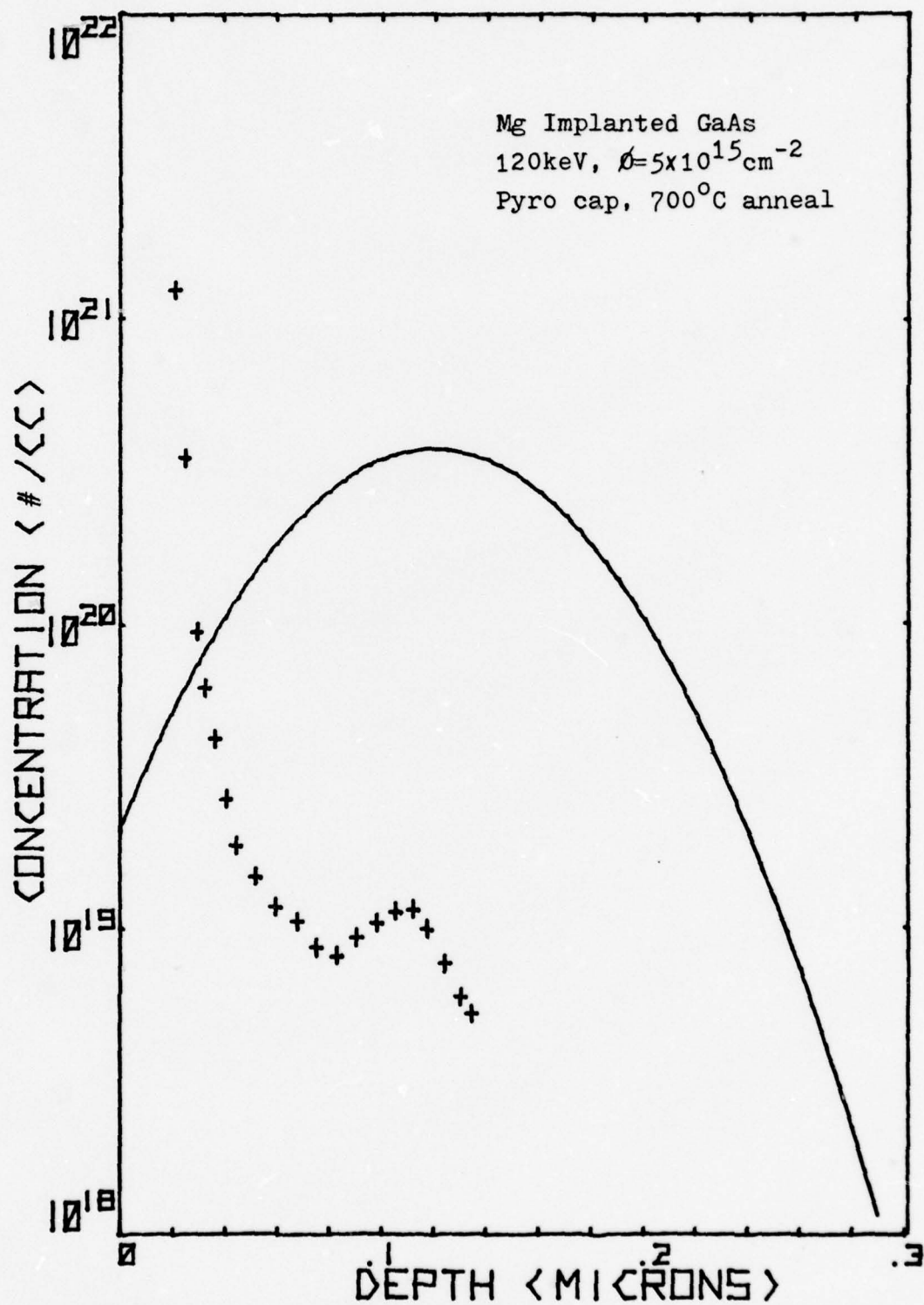Compared to Theoretical LSS Profile

Figure 18.   Measured Profile of Annealed Mg Implanted
GaAs Compared to Theoretical LSS Profile

48

in Figure 19. The large surface concentration is still present and appears to have diffused into the sample. The secondary peak also appears to have indiffused and its magnitude is somewhat smaller than previously observed.

Two samples were implanted at 60keV in order to determine if implant energy was a factor in the observed large surface concentration of pyrolytically capped samples. Figure 20 shows one of the samples annealed at 700°C for 15 min. Again a large surface concentration was observed and the secondary peak was again coincident with the LSS predicted peak. The observed peak surface concentration was larger than the 120 keV implanted samples as expected since the LSS peak is also larger for the 60 keV implants. However, the observed secondary peak concentration was again 1×10^{19} instead of a slightly higher value expected.

The second 60 keV implanted sample is shown if Figure 21. This sample was annealed at 900°C for 15 min. The large surface concentration has shifted somewhat due to indiffusion and the secondary peak has also diffused into the wafer.

The sample shown in Figure 22 was prepared in order to determine the effects of etching off a pyrolytic Si_3N_4 cap as is commonly done for purposes of electrical measurments such as Hall-effect. For this method, a cap is commonly deposited for purposes of annealing and then etched off in fifty percent hydrofluoric acid.

Figure 19. Measured Profile of Annealed Mg Implanted GaAs Compared to Theoretical LSS Profile

50

Mg Implanted GaAs
60keV, $\phi=5\times10^{15}\mathrm{cm}^{-2}$
Pyro cap, 700°C anneal

CONCENTRATION (#/CC)

10^{22}

10^{21}

10^{20}

10^{19}

10^{18}

0　　　　　.1　　　　　.2　　　　　.3
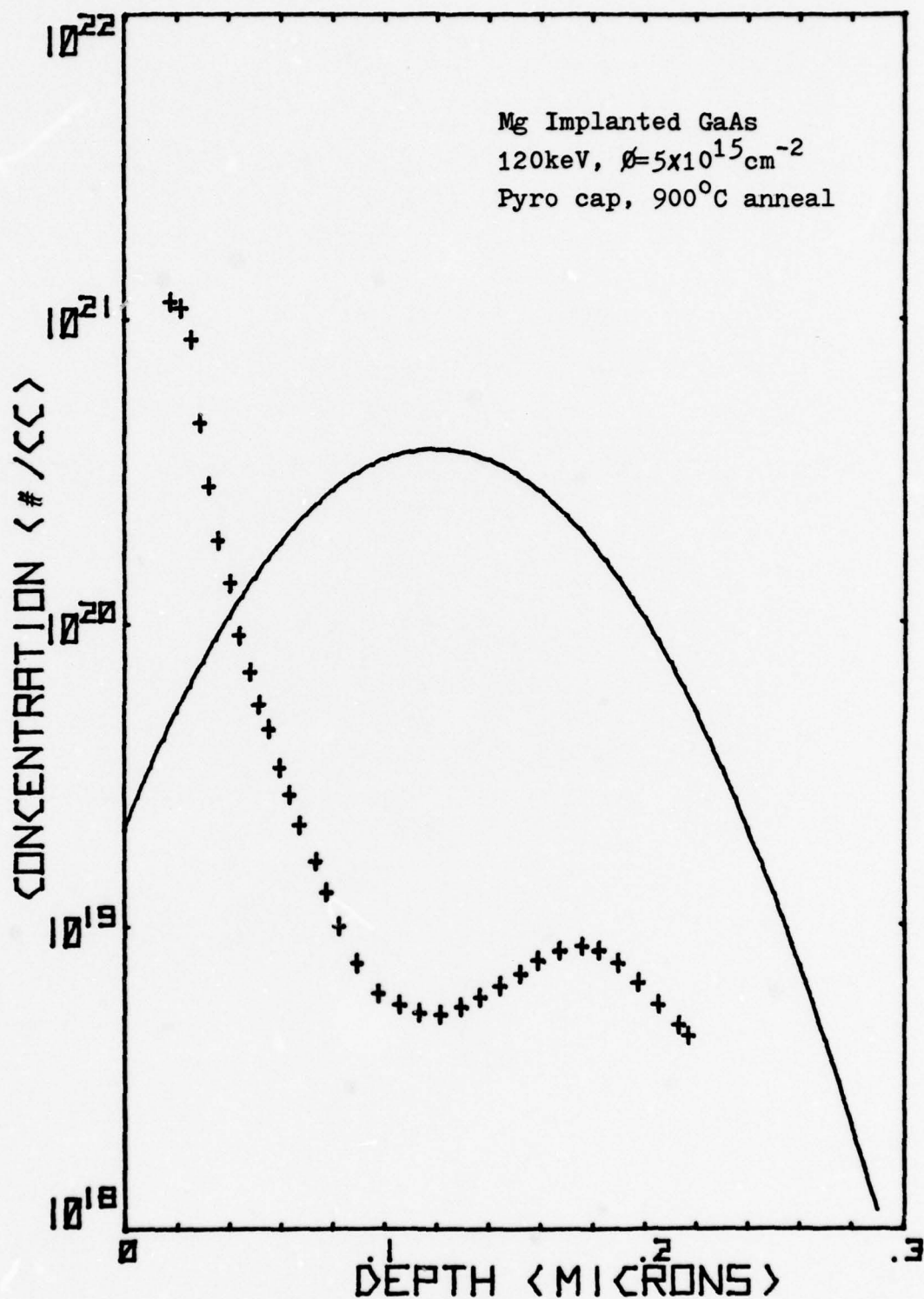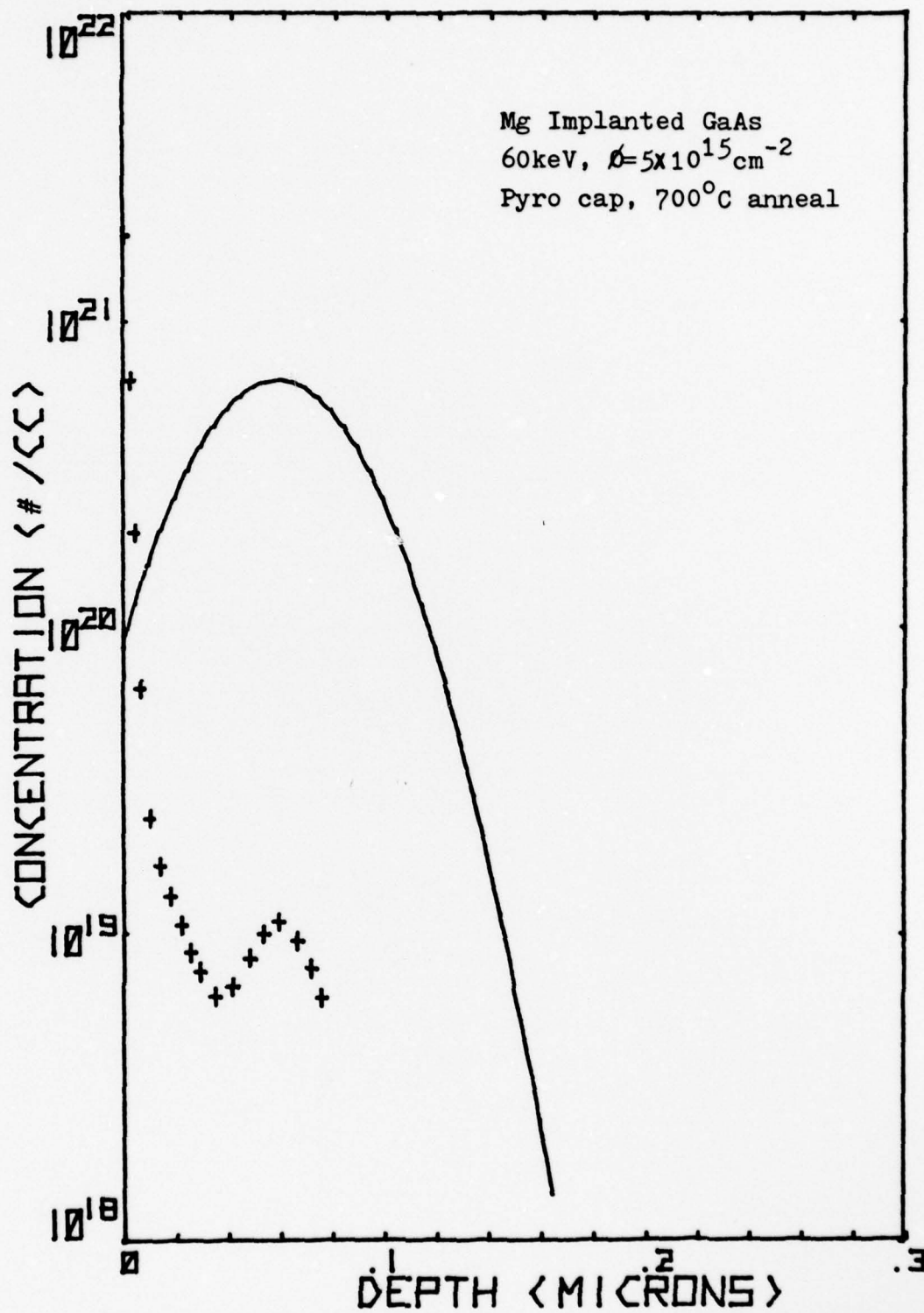DEPTH (MICRONS)

Figure 20.　Measured Profile of Annealed Mg Implanted
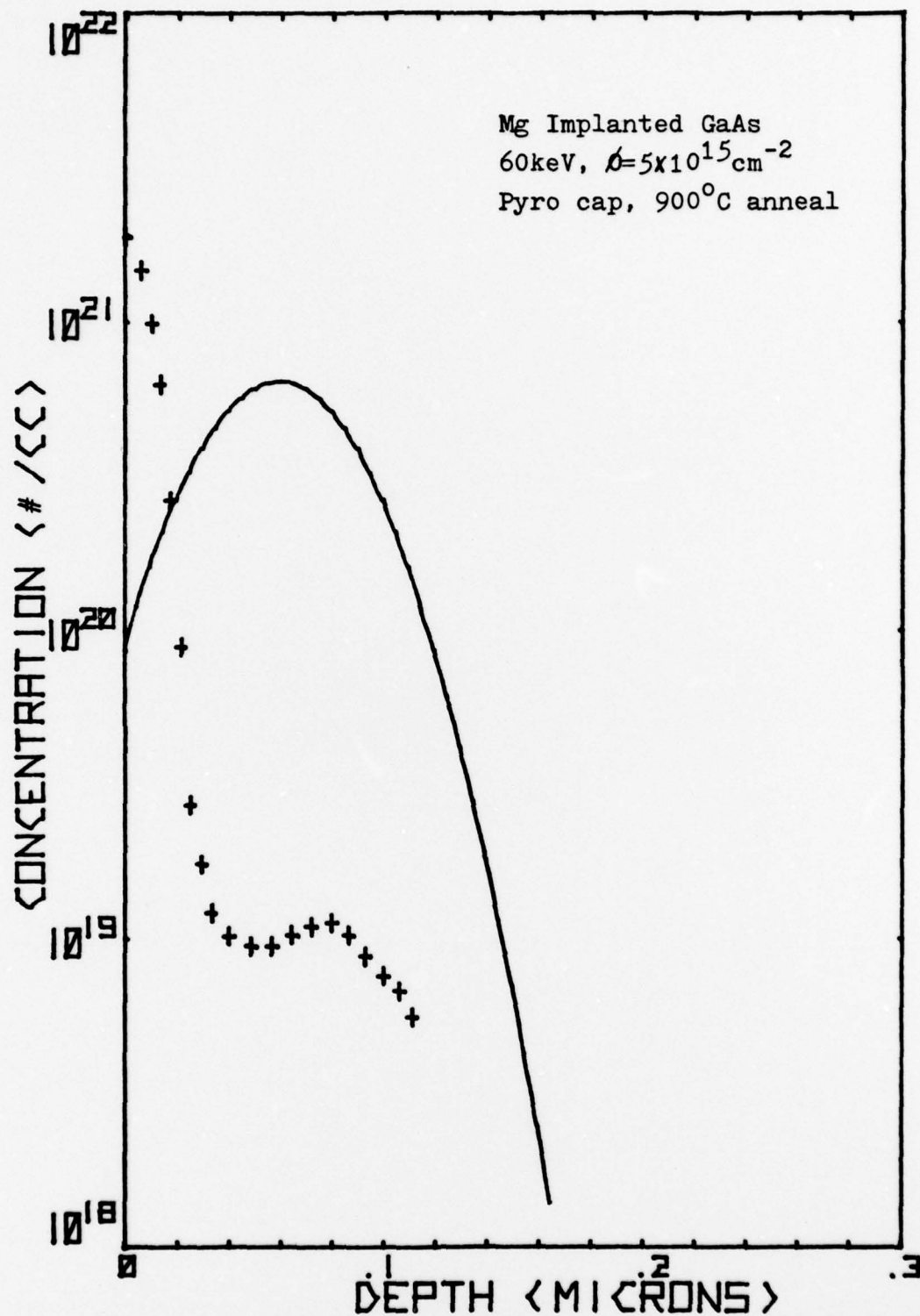GaAs Compared to Theoretical LSS Profile

51

Figure 21. Measured Profile of Annealed Mg Implanted GaAs Compared to Theoretical LSS Profile
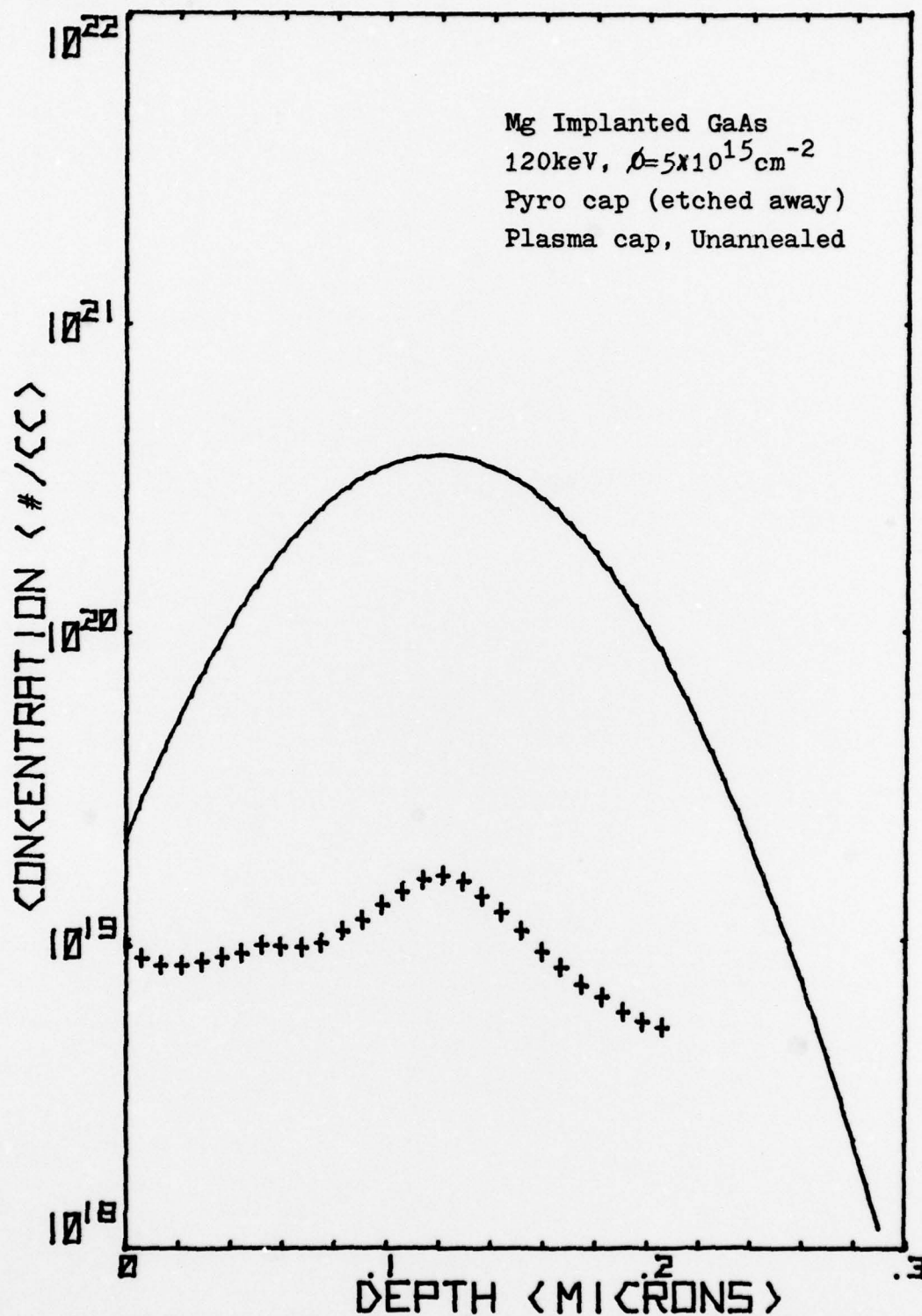
Figure 22. Measured Profile of Mg Implanted GaAs
Compared to Theoretical LSS Profile

The sample was implanted at 120keV on the same target as the sample in Figure 17. It was capped with a 1000Å Si$_3$N$_4$ pyro cap. The cap was then etched away. Following this a 1000Å plasma Si$_3$N$_4$ cap was deposited for purposes of sputtering. The expected profile is expected to be similar to that of Figure 17 since theoretically HF does not attack GaAs. From Figure 22 it is apparant that the large surface concentration is missing and only a much smaller concentration remains. A possible explanation of this observation is that the HF solution dissolves the magnesium in the first few monolayers without affecting the GaAs substrate.

Boron Implants

Boron was implanted in two samples at energies of 60keV and 120keV. These samples were 0.75 cm square and no cap was required. Baseline data was obtained for a 0.75 cm square unimplanted substrate and was subtracted from the impurity profiles for all boron implanted samples. As shown in Figure 23, resulting impurity profiles agree very closely with the LSS calculated profiles. The measured projected range of 1450Å for the 60keV implanted sample agrees favorably with the LSS calculated range of 1513Å. The measured projected range of 2875Å for the 120keV implanted sample is less than the LSS calculated range of 3047Å. The most probable cause can be ascertained by observing the substrate monitor. The intensity of sputtered gallium gradually increases with sputtering time although the increase is very
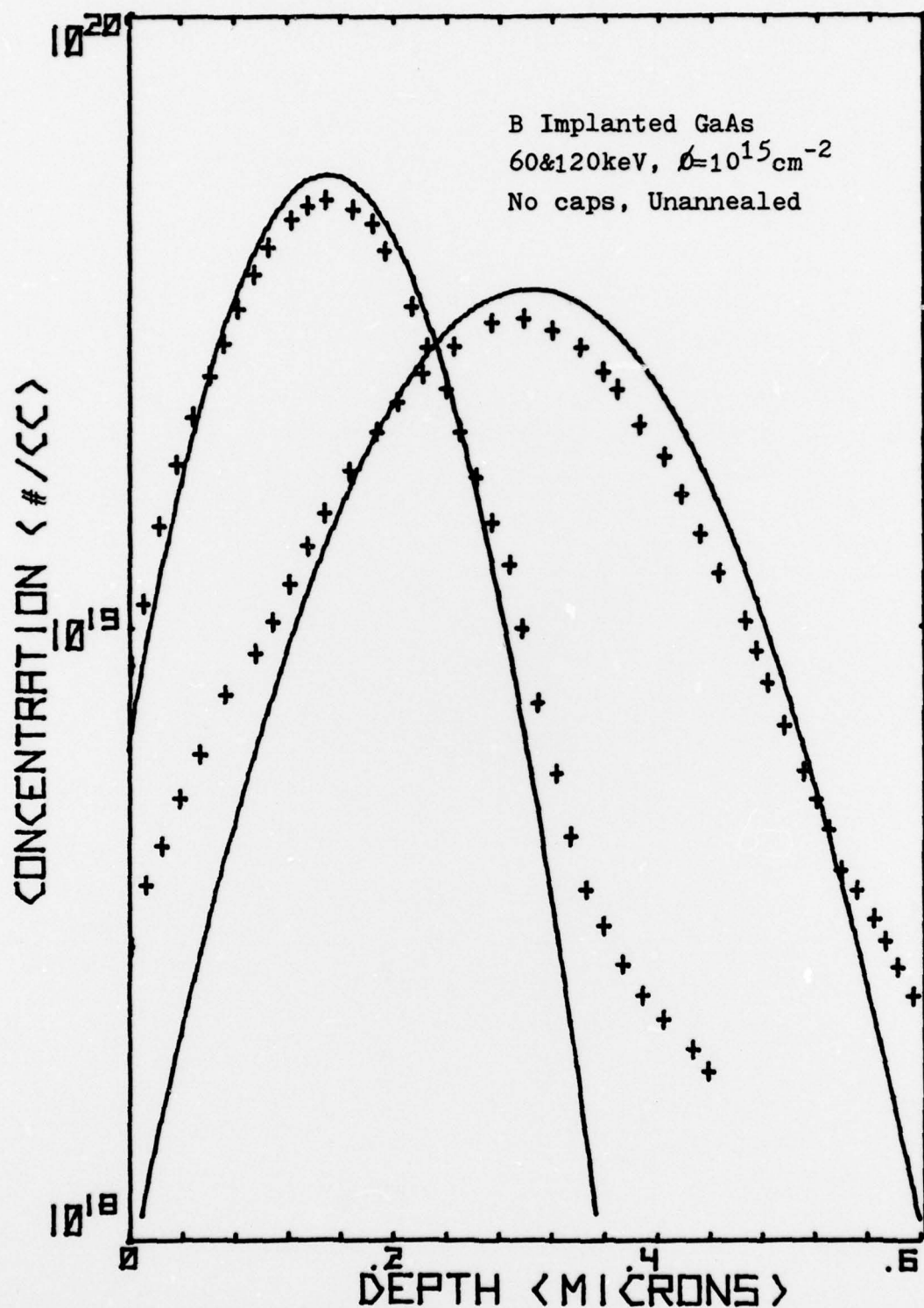
54

Figure 23. Measured Profile of B Implanted GaAs
Compared to Theoretical LSS Profiles

55

slight. This increase corresponds to a slight increase in sputtering rate thus for relatively deep implants the measured profile appears to shift toward the surface.

The sample shown in Figure 24 was implanted with multiple energies of 60keV and 120keV. The predicted concentration profile shown was obtained by adding the individual profiles for the two energies. The resulting measured impurity distribution compares very favorably with the prediction. Again the the trailing edge of the impurity distribution appears to be shifted toward the surface due to the slightly increased sputtering rate.

The effect of annealing on relatively deep implants is shown in Figure 25. The sample was implanted at 120keV, capped with a 1000$\overset{o}{A}$ Si_3N_4 plasma cap, then annealed at 850°C for 15 min. A slight but noticeable increase in surface concentration is most probably due to outdiffusion. As with other annealed samples,the impurity profile has broadened and flattened out, thus the measured peak is lower than the LSS prediction.
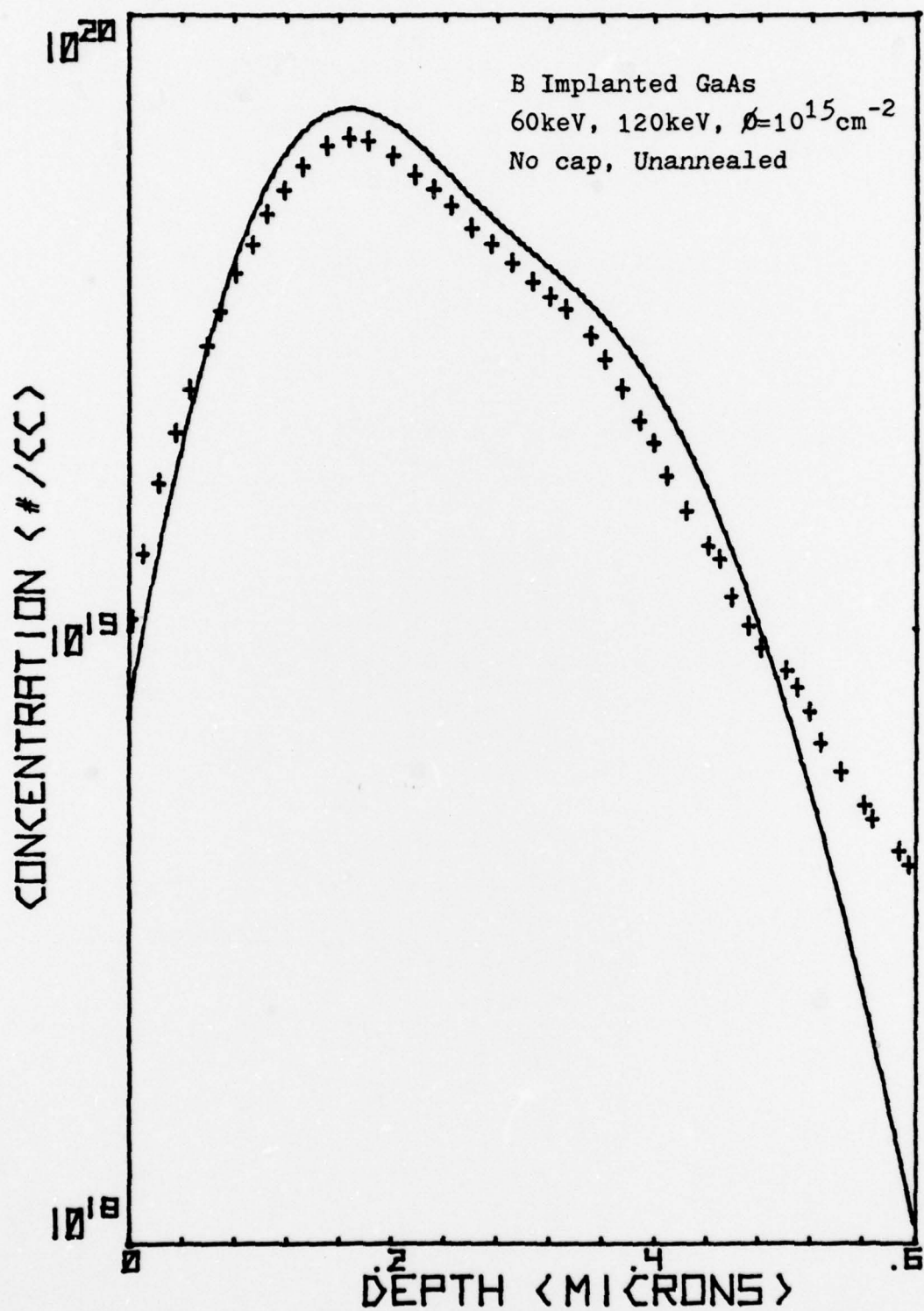
Figure 24. Measured Profile of B Implanted GaAs
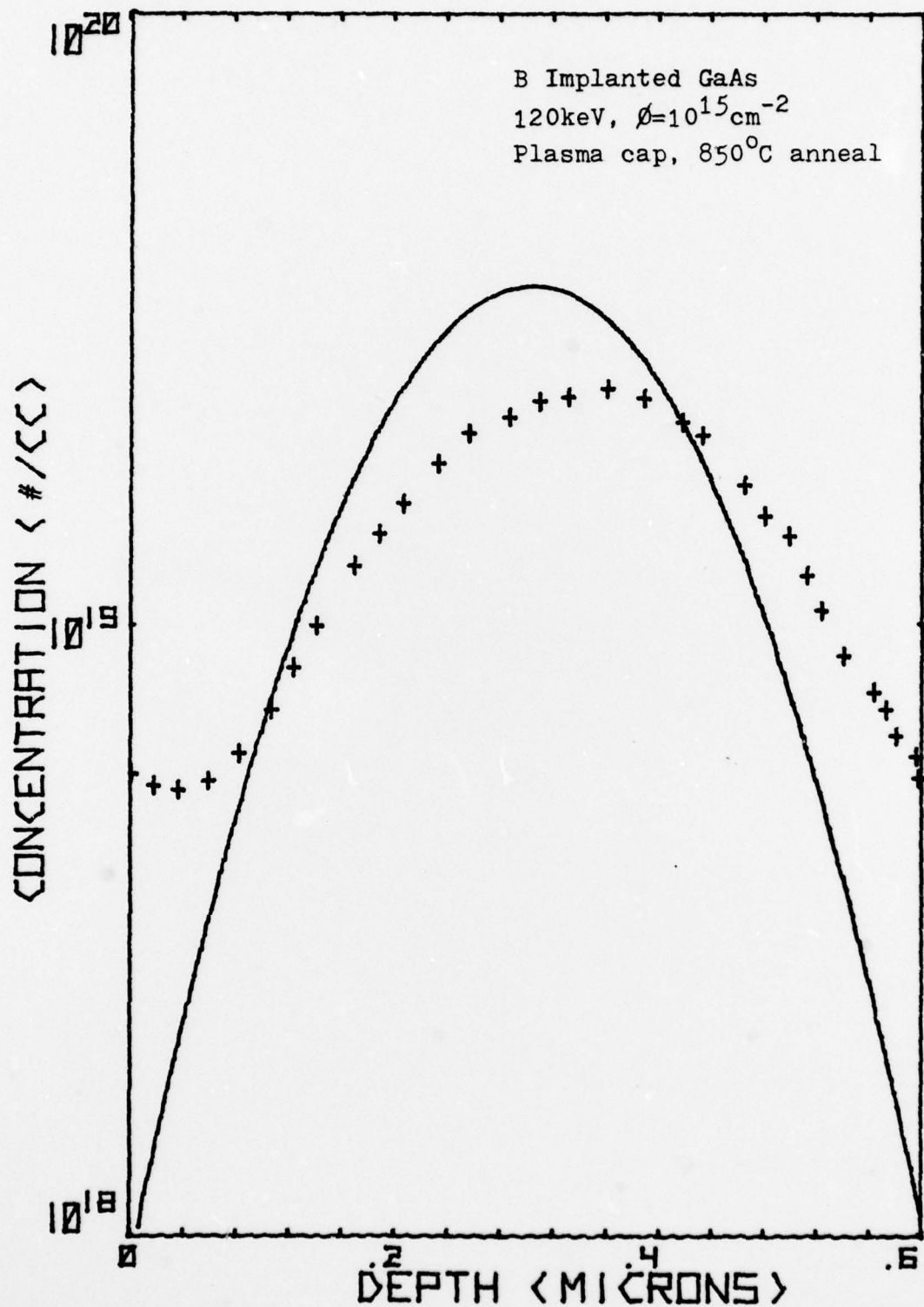(Multiple Energies) Compared to Sum of
Theoretical LSS Profiles

57

Figure 25. Measured Profile of Annealed B Implanted
GaAs Compared to Theoretical LSS Profile

VII Conclusions and Recommendations

Conclusions

After analysis of the experimental results, the fol-
lowing conclusions can be drawn concerning the use of GDOS
for measuring concentration profiles in GaAs:

1. GDOS is an excellent technique for measuring
selected impurity profiles provided several requirements are
met. The first requirement is that the element of interest
must sputter well. Elements such as sulfur that do not
sputter well are not suited to the GDOS technique. The
second requirement and perhaps most important at this time
is that the ion dose or influence must be at least $5 \times 10^{14}/cm^2$.
This leads to high doping concentrations not characteristic
of most devices. The minimum concentration detection limit
of the present system is approximately 10^{18} ions/cm^3.

2. Best results are obtained when larger uncapped
samples are used. A sample size of .75 cm square was deter-
mined to be the optimum size for sputtering. Also capping
samples may lead to undesired results such as outdiffusion
for certain elements like magnesium which have high diffusion
coefficients. For studies of annealed structures, capping
in necessary for the GDOS technique.

3. A high quality plasma Si_3N_4 cap appears to be
superior to a pyrolytic Si_3N_4 cap when capping is necessary.
The $400^{\circ}C$ temperature of the plasma (as compared to $700^{\circ}C$
for pyrolytic deposition) appears to have less effect on

59

implanted ions, as could be expected from the strong dependence on temperature of impurity diffusion coefficients.

4. An accurate calibration of the GDOS system can be accomplished for selected elements if the pure element is available in wafer form. This calibration method was very effective for germanium and boron but less effective for magnesium. It is absolutely essential that all variables in the GDOS system remain constant between the time of calibration and profiling. Any change in parameters (e.g. pressure or optical alignment) will adversely affect calibration.

Recommendations

This investigation has expanded previous studies of the GDOS profiling technique. Futher study should result in lower concentration detection limits. The following recommendations are made for further improvements of the GDOS system:

1. The detection sensitivity should be increased by more efficient light collection. The f number of the quartz lens should be matched to the f number of the spectrometer. Additionally, an investigation should be conducted to determine if rotating the spectrometer 90° so that the entrance slit is parallel to the sample will improve the light collection efficiency.

2. An attempt should be made to increase the efficiency of the excitation process in the discharge chamber in order to increase emission line intensities. Greene,

60

et al, (Ref 15) have reported that the sensitivity of GDOS can be enhanced by mixing small amounts of He (one to five percent) with the Ar sputtering gas.

Bibliography

1. Gibbons, J.F. "Ion Implantation in Semiconductors-Part I: Range Distribution Theory and Experiments." IEEE Proceedings, 56: 295-319 (March 1968).

2. Lindhard, J., M. Scharff, and H. Schiott. "Range Concepts and Heavy Ion Ranges." Kongelige Danske Videnskabernes Selskab, Matematisk-Fysiske Meddelser, 33: 1-39 (1963).

3. Mayer, J.W., L. Erilsson, and J.A. Davies. Ion Implantation in Semi-conductors. New York: Acadmic Press, 1970.

4. Dearnaley, G. et al, Ion Implantation, New York: American Elsevier Publishing Co. Inc., 1973.

5. Papoular, R., Electrical Phenomena in Gases, New York: American Elsevier Publishing Co. Inc., 1965.

6. Cobine, J.D. Gaseous Conductors. New York: Dover Publications, Inc., 1958.

7. Townsend, P.D., J. Kelly, and N. Hartley, Ion Implantation, Sputtering and Their Applications, New York: Academic Press Inc., 1976.

8. Coburn, J., W.E. Taglauer, and E. Kay, "Glow Discharge Mass Spectroscopy Technique for Determining Elemental Composition Profiles in Solids," Journal of Applied Physics, 45: 1779-1786 (1974)

9. Cooper, C.B., R.G. Hart, and J.C. Riley, "Low-Energy Sputtering Yield of the (111) and (111) Faces of GaAs", Journal of Applied Physics, 44: 5183-5184 (Nov 1973)

10. Anderson, G.S. "Atom Ejection in Low-Energy Sputtering of Single Crystals of fcc Metals and of Ge and Si," Journal of Applied Physics, 33: 2017-2025, (Mar 1962)

11. Marcyk, G.T., "GDOS for Measurement of Boron Implanted Distributions in Silicon." Univ. of Illinois, Urbana, Illinois: Thesis (March 1976).

12. Green, J.E. and J.M. Whelan, "Glow-Discharge Optical Spectroscopy for the Analysis of Thin Films." <u>Journal of Applied Physics</u>, <u>44</u>: 2509-2513 (June 1973).

13. Marcyk, G.T. and B.G. Streetman, "Glow Discharge Optical Spectroscopy Measurements of As Implanted Si," <u>Journal of Vacuum Science Technology</u>, <u>14</u>: 1165-1167 (Sep 1977)

14. Gibbons, J.F., W.S. Johnson, and S.W. Mylroie. <u>Projected Range Statistics</u>. (Second Edition). Stroudsburg, Pennsylvania: Halsted Press, 1975.

15. Greene, J.E. et al., "GDOS for Microvolume Elemental Analysis," <u>Journal of Applied Physics</u>. <u>46</u>: 2707 (1975)

Vita

Kenneth R. Williamson was born on 1 July 1950 in New Orleans, Louisiana. Upon graduation from West Jefferson High School in 1968, he attened the University of Southwestern Louisiana from which he received a Bachelor of Science degree in Electrical Engineering, in 1972. He entered Officers Training School in June 1972 and was commissioned as a Second Lieutenant on 20 September 1972. He then attended Pilot Training at Vance Air Force Base, Oklahoma, but was medically eliminated. In October 1973 he was assigned to the 6595th Missile Test Group, Vandenberg Air Force Base, California, where he served as Launch Director for Minuteman III Research and Development Missiles. He departed Vandenberg Air Force Base in June 1977, to enter the School of Engineering, Air Force Institute of Technology.

Permanent Address: 3414 Moss Street
                    Lafayette, Louisiana 70501

SECURITY CLASSIFICATION OF THIS PAGE (When Data Entered)

REPORT DOCUMENTATION PAGE		READ INSTRUCTIONS BEFORE COMPLETING FORM
1. REPORT NUMBER AFIT/GE/EE/78-46	2. GOVT ACCESSION NO.	3. RECIPIENT'S CATALOG NUMBER
4. TITLE (and Subtitle) GLOW DISCHARGE OPTICAL SPECTROSCOPY OF ION IMPLANTED GALLIUM ARSENIDE		5. TYPE OF REPORT & PERIOD COVERED MS Thesis
		6. PERFORMING ORG. REPORT NUMBER
7. AUTHOR(s) Kenneth R. Williamson Capt USAF		8. CONTRACT OR GRANT NUMBER(s)
9. PERFORMING ORGANIZATION NAME AND ADDRESS Air Force Institute of Technology (AFIT-EN) Wright-Patterson AFB, Ohio 45433		10. PROGRAM ELEMENT, PROJECT, TASK AREA & WORK UNIT NUMBERS
11. CONTROLLING OFFICE NAME AND ADDRESS Electronics Research Branch (AFAL/DHR) Air Force Avionics Laboratory Wright-Patterson AFB, Ohio 45433		12. REPORT DATE December, 1978
		13. NUMBER OF PAGES 64
14. MONITORING AGENCY NAME & ADDRESS(if different from Controlling Office)		15. SECURITY CLASS. (of this report) Unclassified
		15a. DECLASSIFICATION/DOWNGRADING SCHEDULE

16. DISTRIBUTION STATEMENT (of this Report)

Approved for public release; distribution unlimited

17. DISTRIBUTION STATEMENT (of the abstract entered in Block 20, if different from Report)

18. SUPPLEMENTARY NOTES

Approved for public release; IAW AFR 190-17

Joseph P. Hipps, Major, USAF
Director of Information   1-23-79

19. KEY WORDS (Continue on reverse side if necessary and identify by block number)

Glow Discharge Optical Spectroscopy
Ion Implantation
Gallium Arsenide
Impurity Concentration Profile

20. ABSTRACT (Continue on reverse side if necessary and identify by block number)

Glow Discharge Optical Spectroscopy (GDOS) was used as a technique for obtaining impurity concentration profiles of annealed and unannealed ion implanted GaAs samples. Germanium, magnesium, and boron ions were implanted at energies of 60keV or 120keV and fluences of $1 \times 10^{15}/cm^3$ or $5 \times 10^{15}/cm^2$. The samples were sputtered in a dc glow discharge. The intensities of strong emission lines (proportional to concentration) were calibrated using pure elements as standards, providing impurity concentration profiles.

DD _{1 JAN 73} FORM 1473   EDITION OF 1 NOV 65 IS OBSOLETE   Unclassified

1 or 5 times 10 to the 15th power /sg. cm.

SECURITY CLASSIFICATION OF THIS PAGE (When Data Entered)